MONTHLY MEAN FORECAST EXPERIMENTS WITH THE GISS MODEL[1,2]

by

Jerome Spar[3], Robert Atlas, and Eugene Kuo

The City College

City University of New York

March 1976

[1]This research was supported by the National Aeronautics and Space Administration, Goddard Space Flight Center, under Grant NGR 33-013-086.

[2]Contribution No. 41, CUNY Institute of Marine and Atmospheric Sciences

[3]Department of Earth and Planetary Sciences

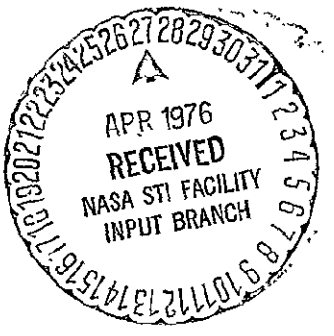

ABSTRACT

The GISS general circulation model is used to compute global monthly mean forecasts for January 1973, 1974, and 1975 from initial conditions on the first day of each month, with ocean surface fluxes based on climatological mean January sea-surface temperatures. Forecasts are evaluated in terms of global and hemispheric energetics, zonally-averaged meridional and vertical profiles, forecast error statistics, and monthly mean synoptic fields. Although it generates a realistic mean meridional structure for the month of January, the model does not adequately reproduce the observed interannual variations in the large-scale monthly mean energetics and zonally-averaged circulation. The model exhibits no general skill in predicting the monthly mean sea-level pressure field, but it does simulate observed changes in the intensity of the Icelandic low from year to year. For each January the model produces a prognostic monthly mean 500-mb height field that is superior to climatology and persistence.

The impact of temporal sea-surface temperature variations on monthly mean global forecasts with the GISS model is investigated by comparing two parallel forecasts for January 1974, one using climatological ocean temperatures for the surface flux computations, and the other observed daily ocean temperatures. In the one case studied, the use of daily-updated sea-surface temperatures produced no discernable beneficial effect on the forecasts, and the total impact on the large-scale pressure and temperature fields was small.

MONTHLY MEAN FORECAST EXPERIMENTS WITH THE GISS MODEL

1. INTRODUCTION

All dynamical weather predictions presently appear to exhibit a similar decay of skill when verified against daily synoptic fields, generally showing little or no superiority over climatology after about 3 to 7 days.[4] (See, e.g., Miyakoda et al., 1969, Baumhefner, 1970; Miyakoda et al., 1972; Druyan, 1974; Spar and Atlas, 1975; Druyan et al., 1975). It has also been shown in a number of theoretical and experimental studies that inherent uncertainties in the initial state of the atmosphere apparently limit the maximum range of deterministic predictability to 2 to 3 weeks. (See, e.g., Smagorinsky, 1969; Lorenz, 1973; Leith, 1974). Nevertheless, despite the limited skill of daily prognostic maps beyond the short range, it is possible that time-averaged numerical predictions may retain some useful skill over longer periods of time. There is some empirical evidence (e.g., Namias, 1953; 1964) that certain large-scale atmospheric anomalies may preserve their identity over periods of a month or even a season, and that time-averaging, by filtering out the smaller-scale and shorter-lived components of the atmosphere and by diminishing the effects of phase errors, may thus yield some detectable skill over extended and long ranges.

The availability of global general circulation models (GCM's) which can be integrated over effectively unlimited time and are theoretically unconstrained by lateral boundary errors provides a tempting opportunity to test this hypothesis. In this study we have computed a set of experimental global monthly mean forecasts for three winter months - January

---

[4] The range of predictability depends upon the variable predicted, being generally shorter, for example, for surface pressure than for 500-mb height.

of 1973, 1974, and 1975 - using the so-called GISS[5] GCM (Somerville et al., 1974). Druyan et al. (1975) have already reported evidence of some skill in a set of two-week averaged forecasts with this model, and the present study may thus be regarded as an extension of their work.

Experiments in monthly prediction lie somewhere in a nebulous region between climate simulation and practical weather forecasting. One does not expect to predict successfully the synoptic details and events that constitute the month's weather, but one does hope that time-averaged properties will be at least realistically simulated. Primarily, these experiments are designed to investigate the degree to which observed gross differences between the January of one year and another are determined by the initial conditions at the beginning of each month and are simulated by the model.

A description of the GISS model may be found in Somerville et al., (1974). It is a global, spherical coordinate (4 degrees of latitude by 5 degrees of longitude),[6] 9-layer, primitive equation, "sigma" coordinate system with upper boundary at 10 mb, integrated in 5-minute time steps using Arakawa's (1972) numerical method[6], and employing Arakawa's (1969) cumulus convection parameterization, parameterized solar and terrestrial radiative fluxes dependent on predicted water vapor and cloud distributions, specified surface boundary conditions[7] but predicted

---

[5] The GISS model was developed at the Goddard Institute for Space Studies, NASA, located in New York City.

[6] In the version of the model used in this study the numerical method was altered to include a "split grid" (Halem and Russel, 1974) in which the longitudinal interval increases discontinuously at higher latitudes. At the same time, Arakawa's TASU (time-alternating, space-uncentered) scheme was eliminated.

[7] Since the publication of Sommerville et al. (1974), the surface albedo in the model has been modified to represent a greater variety of surface conditions. The climatological January albedo distribution used in the present study was taken from Schutz and Gates (1972) and is based on the original data of Posey and Clapp (1964).

surface land temperatures, and parameterized surface fluxes of heat, water vapor, and momentum. A mean state computed by the model for January 1973 from initial data for 20 December 1972 has already been published in Somerville et al. (1974) where it is compared with the January 5-year climatology of Oort and Rasmusson (1971). The mean states computed for the present study were all initialized on 1 January (00 GMT), and each is verified against the observed mean January state for the same year.

As shown by Somerville et al. (1974), the model produces a realistic, albeit imperfect, simulation of the mean January troposphere. The model stratosphere is less satisfactory, probably due to the poor vertical resolution at high levels. Even in the troposphere the model exhibits certain defects: the winter polar regions are too cold, meridional circulations are too weak, westerly jets are too broad, horizontal gradients are too weak, and eddy energies are too small. The model is still in the process of development. However, even at this stage, it appears to generate a sufficiently credible meteorological history to justify a mean monthly forecast experiment, and it is apparently representative of the current "state of the art" of numerical weather prediction (Druyan, 1974).

Two related experiments are described in this paper. In the first, a set of three monthly mean forecasts was computed from 12-hourly outputs of the GISS model for January of 1973, 1974 and 1975. All three forecasts used the same fixed sea-surface temperature (SST) field, corresponding to the climatological SST field for January (from Washington and Thiel, 1970), but each was, of course, started from different initial atmospheric conditions. These three forecasts are discussed in section 2. In the second experiment, described in section 3, boundary con-

ditions, rather than initial conditions were varied. The latter experiment, which was designed to evaluate the effect of temporal SST variations on the monthly mean forecasts, was, however, carried out only for January of 1974. In this study, two parallel forecasts for January 1974 were computed from the same initial atmospheric conditions, but with different SST fields, one forecast using the climatological field and the other an observed SST field that was updated daily.

The global data sets used for both initialization and verification of the forecasts were provided by the National Meteorological Center (NMC) and interpolated into the GISS grid. The January 1973 and 1974 data were derived from a combination of the then-operational NMC analysis north of latitude 18N and a Flattery spectral Hough function analysis (Flattery, 1971; National Weather Service, 1974) over the rest of the globe. For the January 1975 data, however, the now-operational Flattery spectral analysis was used over the entire globe.

After the experiment was completed, it was learned from NMC that an error[8] had been committed in all the 12 GMT analyses for January 1975. Therefore, these data were subsequently discarded, and all the January 1975 observed means were recomputed solely from the 24-hourly 00 GMT NMC analyses. Thus, the "observed" January 1975 mean values and energetics were computed from 00 GMT data only, while the forecast mean values for all three months were computed by 12-hourly averaging of both 00 and 12 GMT outputs. However, in order to assess the effect of 24-hourly vs. 12-hourly averaging, the forecast mean values for January 1975 were computed both ways, and are discussed below.

---

[8] In the "first guess" for all 12 GMT analyses during this period, data for 6 October 1974 were erroneously accessed. This error was not corrected until 4 February 1975, according to NMC staff (personal communication).

Another, presumably minor, inconsistency also was committed in the SST update experiment for January 1974. In this calculation, the two parallel forecasts (one with the climatological SST and one with the daily updated SST) were computed using a slightly earlier and different version of the GISS model. Specifically, the model used in the SST update experiment employed an older and somewhat less satisfactory code for the long-wave radiation computations, as well as the original specification of surface albedo, with its smaller spatial variability (see footnote 7). Thus, the January 1974 forecast reported in section 3 below, is not quite the same as the January 1974 forecast described in section 2. However, in view of the fact that the SST update experiment was intended primarily to reveal the impact of temporal SST variations and anomalies on the monthly forecasts, and considering other deficiencies of the model as a forecasting system, the inconsistency in the January 1974 computations between sections 2 and 3 is probably of trivial consequence.

2. EVALUATION OF THREE JANUARY FORECASTS

In this section we examine the interannual variations of the observed January atmospheres, as they are represented by the NMC analyses, as well as the corresponding variations in the predicted January mean atmospheres as computed by the GISS model. The forecast and observed mean January states are compared for each of the three years separately. As noted above, the three January forecasts were computed with the same model and identical boundary conditions. They therefore differ only because of the different initial conditions on 1 January of each year. Agreement between the forecast and observed atmospheres would signify (a) that the differences among the observed mean January states are determined by the initial conditions, and (b) that the model correctly simulates this dependence. Disagreement could indicate that either one or both of these statements is false, or alternatively, that, perhaps due to defects in the observation and analysis system, the apparent differences among the "observed" Januarys may not be real.

The evaluation of the monthly forecasts is presented below in four sub-sections devoted to the energetics of the mean atmosphere, mean meridional and vertical profiles, forecast error statistics, and monthly mean synoptic maps. Although the forecasts were computed over the entire globe, only the results for the Northern Hemisphere are discussed in any detail. Some global data are presented, but our confidence in the global statistics is much lower than in the results for the Northern Hemisphere, where most of the observational data are concentrated.

Energetics

Because of the known deficiencies of the model stratosphere, the energetics of the predicted and observed atmospheres are computed only for the tropospheric region represented by the lower 8 layers of the model (i.e., up to about 120 mb), as in Somerville et al. (1974). The forecast

(F) and observed (O) energetics for each January, as well as the 3-year averages, together with recent "climatological"[9] estimates of January energetics for the Northern Hemisphere by Peixoto and Oort (1974) and Oort and Peixoto (1974), are presented in Table 1. (The climatological energetics were computed in the mixed space-time domain, while the forecast and observed energetics from this study shown in Table 1 were computed in the space domain. However, as noted by Oort and Peixoto (1974) and discussed by Tenenbaum (1976), the differences between the two methods of computation are considered to be small compared with errors from all other sources). The energies are given in units of 10^5 Joules meter^{-2} (J m^{-2}) and the energy conversions in Watts meter^{-2} (W m^{-2}). Mean zonal available potential energy and zonal kinetic energy are represented by P_M and K_M, respectively, while the corresponding eddy energies are denoted by P_E and K_E[10]. Energy conversions, P_M/K_M, P_M/P_E, P_E/K_E and K_E/K_M, are positive when the conversion is from the first form to the second form, and negative if in the opposite sense. Global energies are also shown in Table 1 for each January together with the 3-year averages. All the energy calculations for this study, both forecast and observed, are based on the spherical grid of 4 degrees of latitude by 5 degrees of longitude, while the "climatological" values are based on an enlarged NMC grid (Oort and Rasmusson, 1971).

---

[9] The "climatological" values are based on 5 years of data, 1959-1963, and are computed by integrating up to the 75 mb level.

[10] Eddy energies include both transient and standing eddies. Thus, this part of the study is concerned not only with the eddy structure of the mean maps, but also with spatial and temporal variations during the month.

Table 1. Forecast (F) and Observed (O) January energetics. Units: energy, 10^6 J m^{-2}; energy conversion, W m^{-2} P_M and P_E are mean zonal and eddy available potential energies; K_M and K_E are mean zonal and eddy kinetic energies. Five-year "climatological" values are from Peixoto and Oort (1974).

(A) Northern Hemisphere

	1973		1974		1975[11]		3-Year Average		1959-1963 Climatology
Energy	F	O	F	O	F	O	F	O	
P_M	61.4	55.5	58.1	54.5	67.5	55.9	62.3	55.3	55.8
P_E	9.0	8.0	8.2	8.8	6.8	7.2	8.0	8.0	10.5
K_M	9.9	9.4	9.5	8.7	10.7	7.8	10.0	8.6	8.0
K_E	6.4	6.9	6.5	7.6	4.7	6.7	5.8	7.1	9.3
Conversion									
P_M/K_M	-1.3	+5.2	-1.1	+6.1	-1.1	+0.4	-1.2	+3.9	-0.1
P_M/P_E	+3.1	+2.2	+1.3	+3.0	+2.3	+2.6	+2.2	+2.6	+2.8
P_E/K_E	+2.5	+4.0	+2.3	+4.4	+2.5	+0.8	+2.4	+3.1	+3.4
K_E/K_M	+0.5	+0.3	+0.1	+0.3	+0.5	+0.3	+0.4	+0.3	+0.3

(B) Globe

	1973		1974		1975		3-Year Average	
	F	O	F	O	F	O	F	O
P_M	45.1	43.1	41.8	44.4	47.3	42.0	44.7	43.2
P_E	6.5	5.2	6.5	5.8	4.9	4.9	6.0	5.3
K_M	7.7	7.3	7.2	7.4	8.0	6.5	7.6	7.1
K_E	5.4	4.5	6.1	5.1	3.8	4.7	5.1	4.8

[11] Due to a computer problem, the January 1975 forecast was run for only 29 days and the observed January 1975 results are for a 30 day period.

The 1975 forecast values listed in Table 1, like all the values for 1973 and 1974, were computed by 12-hourly averaging, using both 00 and 12 GMT outputs, whereas, for reasons explained above, the 1975 observed values are based on 24-hourly averaging of the 00 GMT analyses only. The differences between the 12-hourly and 24 hourly averaged forecast mean energetics are, however, generally insignificant, as shown in Table 2. Also shown in Table 2 are the 12-hourly averaged observed mean energetics (including the effects of the contaminated 12 GMT analyses for which the wrong first guesses were used) compared with the 24-hourly averaged (00 GMT only) observed means. The combined effect of both the analysis error and the sampling interval on the observed mean energetics is also seen to be relatively small. Thus, in view of the data in Table 2, the effect of sampling interval on the results shown in Table 1 may be ignored.

Compared with the 5-year January climatology for the Northern Hemisphere, the average observed January data in Table 1 for the 3-year period 1973-1975 appear to exhibit relatively low eddy energies, which may or may not be the result of differences in methods of analysis and computation (Tenenbaum, 1976). (The use of space vs. space-time domain energetics accounts for only a trivial part of the difference between the two periods). The average observed zonal energies, on the other hand, are in fairly good agreement with the values from Peixoto and Oort (1974). The observed conversion rates for the 3-year period are also in good agreement with the 5-year climatology, with the exception of the P_M/K_M conversion, which is generally considered to be unreliable (Tenenbaum, 1976).[12]

[12] A more comprehensive diagnosis of the GISS model's energetics, including a spectral analysis, may be found in Tenenbaum (1976).

Table 2. Comparison of 12-hour averaged (00 and 12 GMT) and 24-hour averaged (00 GMT only) monthly mean energetics for January 1975. (See Table 1 and text for explanation of symbols).

	F		O	
	12-hour	24-hour	12-hour	24-hour
Energy		Northern Hemisphere		
P_M	67.5	67.5	55.5	55.9
P_E	6.8	6.8	7.2	7.2
K_M	10.7	10.7	7.8	7.8
K_E	4.7	4.7	6.3	6.7
Conversion				
P_M/K_M	-1.1	-0.7	+0.4	+0.4
P_M/P_E	+2.3	+2.3	+2.5	+2.6
P_E/K_E	+2.5	+2.4	+0.6	+0.8
K_E/K_M	+0.5	+0.4	+0.3	+0.3
Energy		Globe		
P_M	47.3	47.4	41.8	42.0
P_E	4.9	4.9	5.1	4.9
K_M	8.0	8.0	6.5	6.5
K_E	3.8	3.8	4.5	4.7

The average forecast zonal potential and zonal kinetic energies for the 3-year period are both higher than observed in the Northern Hemisphere. Forecast and observed zonal energies are in closer agreement, however, in the Southern (summer) Hemisphere, and the effect of this is reflected in the global values shown in Table 1. The 3-year average forecast eddy potential energy is in good agreement with the corresponding observed value in the Northern Hemisphere, but the forecast eddy kinetic energy is too low. On the other hand, the forecast eddy energies are higher than "observed" in the Southern Hemisphere, and the effect of this is also reflected in the tabulated global values. However, it appears quite likely that the low eddy energies apparently observed in the Southern Hemisphere may be simply the result of data paucity and excessive smoothing in the analysis. The average forecast conversion rates (except for P_M/K_M) are in reasonable agreement with the observed values.

In the Northern (winter) Hemisphere, the model tends to overpredict the mean meridional temperature gradient each January, and hence also the mean zonal potential and kinetic energies. (For example, the average vertically-integrated mean temperature difference between latitudes 10 N and 70 N is forecast to be 30^0 K and observed to be 26^0 K for the 3-year period). As shown by Stone et al. (1975), this defect in the model is apparently due to an underestimate of the influx of sensible heat to high latitudes by large eddies, as a result of which the Arctic regions are forecast to be too cold in winter. The model also consistently underpredicts the eddy kinetic energy each year in the Northern Hemisphere, a defect apparently common to all coarse-grid GCM's.

The interannual variations of zonal available potential energy predicted by the model are much larger than observed in the Northern Hemisphere. As measured, for example, by their mean deviations, the

forecast and observed values of P_M in the Northern Hemisphere vary by 3.4 and 0.5 ($\times 10^5$ J m^{-2}), respectively, over the three Januarys. (The corresponding standard deviations are about twice as large.) For each of the other energy forms, the interannual variabilities of the forecast and observed values are more alike, with forecast and observed mean deviations (in units of 10^5 J m^{-2}) of 0.8 and 0.5 for P_E, 0.4 and 0.8 for K_M, and 0.8 and 0.4 for K_E, respectively. Thus, the model appears to forecast greater interannual variability of P_M, P_E, and K_E than observed, but less variability of K_M. The latter result, however, is due primarily to the relatively low value to which the observed K_M fell in January 1975. From simple geostrophic (thermal wind) considerations, one would expect P_M and K_M to rise and fall together, as both depend on the meridional temperature gradient. However, in January 1975, the observed value of P_M in the Northern Hemisphere rose to its maximum for the 3-year period, while that of K_M fell to its minimum level. While this curious result could be an effect of the non-linear dependence of K_M on wind speed, it is worth noting that the forecast values of P_M and K_M do show the expected parallel variations of P_M and K_M from year to year. The observed values of both K_M and P_M in January 1975 are actually closer to the 5-year climatological values than are those of the prior two years, and therefore cannot be rejected as anomalous. Nevertheless, the possibility exists that errors in the estimates of P_M or K_M, either in 1975 or in the prior two years, could account for the lack of parallel variation of the observed values.

The forecast for January 1975 gives anomalously high values for the zonal energies and low values for the eddy energies (particularly kinetic) in the Northern Hemisphere. The observed eddy energies in January 1975 are, in fact, low for the 3-year period (and much lower than the climatological values), although not as low as predicted. Thus, the model appears to indicate correctly the sign of the negative eddy energy anomaly in 1975, but overpredicts its magnitude.

In general, the model appears to forecast somewhat larger energy fluctuations than are observed from year to year over the Northern Hemisphere. It fails to reproduce consistently the observed pattern of interannual energy variations, indicating the correct sign of the interannual change for P_M and K_E over the 3-year period, but the wrong sign half the time for K_M and P_E.

Meridional and Vertical Profiles

Forecast (F) and observed (O) meridional profiles of the mean zonal circulation for each January are shown in Fig. 1 as dashed and solid curves, respectively, plotted as functions of latitude from pole to pole. The mean zonal winds, in meters sec^{-1}, are averaged over pressure (height) as well as longitude at intervals of 4 degrees of latitude, and include all 9 layers of the model. For reference, the climatological 5-year mean zonal winds, taken from Oort and Rasmusson (1971), are also shown (as crosses) for the region between latitudes 10 S and 75 N. (Positive values denote westerlies, negative values easterlies).

It is apparent from Fig. 1 that the model simulates the general configuration of the mean zonal wind profile rather realistically over

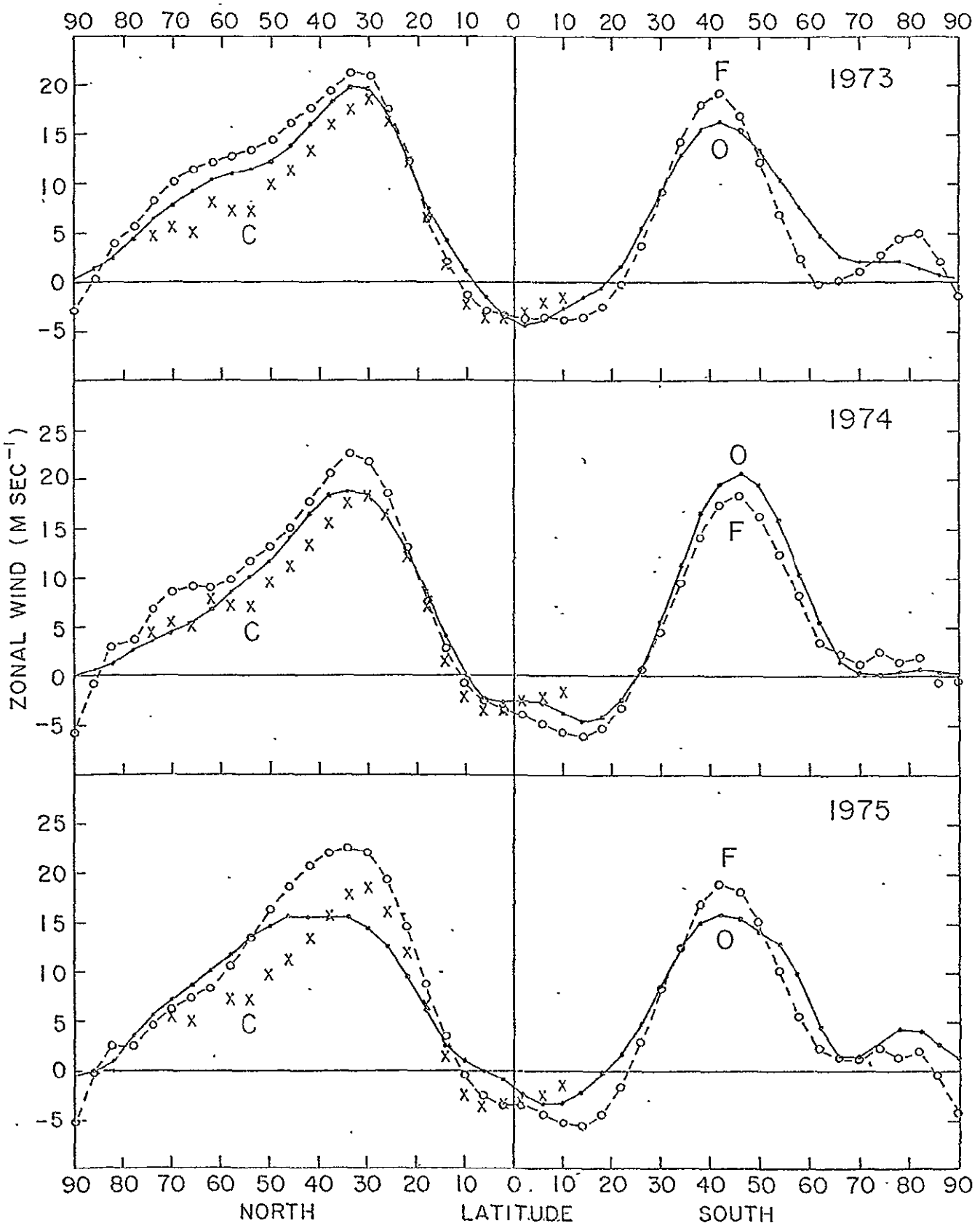
90 80 70 60 50 40 30 20 10 0 10 20 30 40 50 60 70 80 90
1973
1974
1975
F
O
C
ZONAL WIND (M SEC⁻¹)
NORTH
LATITUDE
SOUTH

FIG.1

the 3 year period, particularly in 1973 and 1974. However, in January 1975 the model fails to predict what appears to be an anomalous observed mean zonal circulation in the Northern Hemisphere, which is characterized by a broad, weak wind maximum shifted poleward relative to the climatological profile. While the maximum observed mean westerlies decreased markedly from January 1973 to 1975, the forecast indicates stronger maximum westerlies in 1975 than in 1973, with little shift in latitude. (On the other hand, the model does correctly simulate the strengthening of the westerlies in January 1975 in the higher middle latitudes of the Northern Hemisphere, and also indicates a somewhat broader maximum than in the previous two years.) The discrepancy in Fig. 1 between the forecast and observed mean zonal wind profiles over the Northern Hemisphere in January 1975 illustrates the source of the difference between the forecast and deserved mean zonal kinetic energies in 1975 noted in Table 1.

In the Southern Hemisphere, where the observed profiles in Fig. 1 appear to indicate a biennial oscillation in the speed of the maximum mean westerlies, the model predicts little or no interannual variation, so that the forecast is out of phase with the observed variation. On the other hand, the interannual shifts in the latitude of the maximum mean westerlies in the Southern Hemisphere are simulated rather well by the model.

As a further illustration of the model's simulation of interannual variations in the large scale circulation, Fig. 2 shows the forecast (F) and observed (O) vertical profiles of the mean zonal wind for

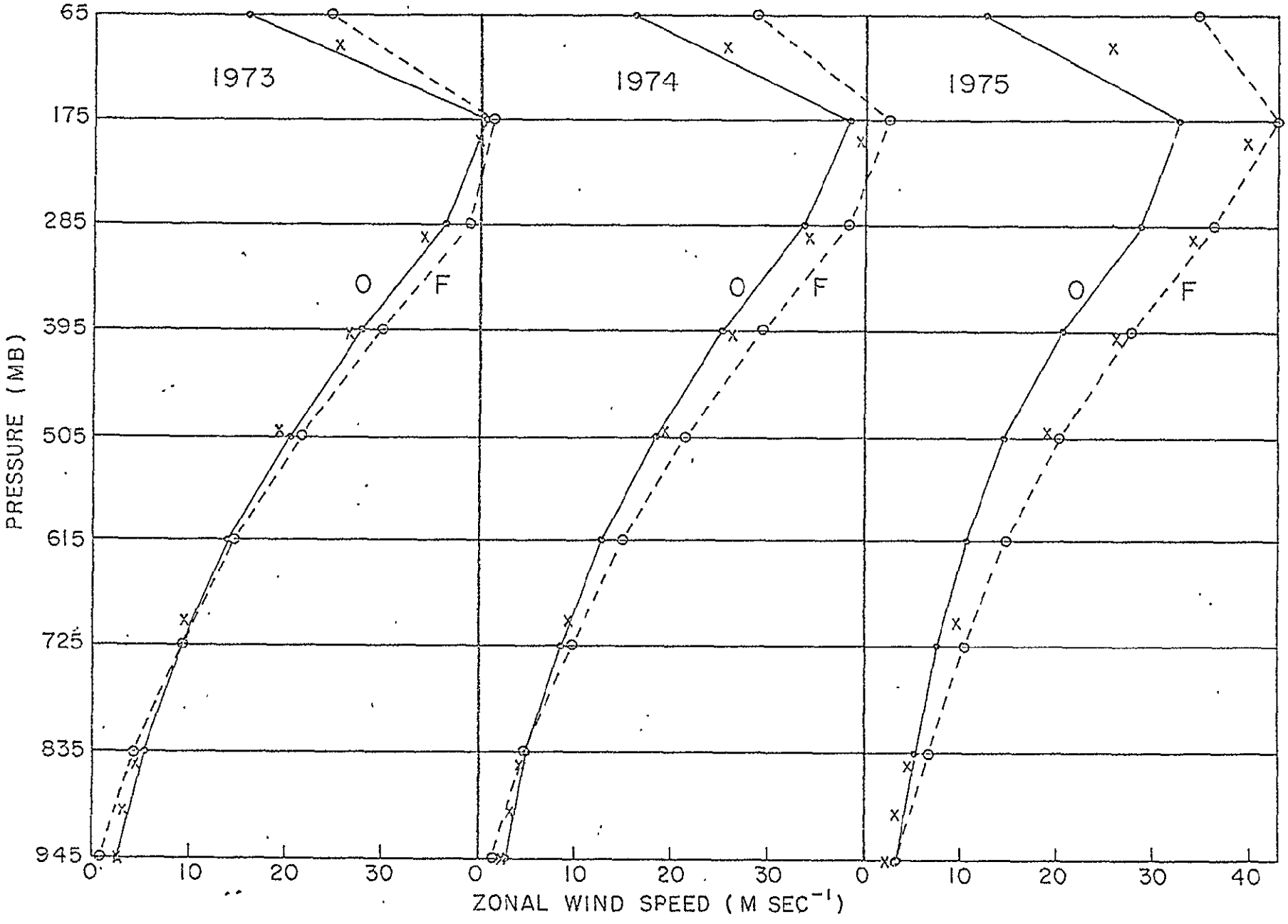
1973
1974
1975
O
F
65
175
285
395
505
615
725
835
945
PRESSURE (MB)
0
10
20
30
40
ZONAL WIND SPEED (M SEC^{-1})

FIG. 2

each January at the latitude of the observed jet stream in the Northern Hemisphere (latitude 30 N in January 1973 and 1974, and 34 N in January 1975). Again, the data from Oort and Rasmusson (1971), in this case for latitude 30 N, are plotted (as crosses) for comparison.

The vertical wind profile, like the meridional profile of the zonal wind, is realistically simulated, in general, by the model over the 3-year period. However, the model fails to reproduce the marked decline in the jet stream velocity from January 1973 to 1975, and, in fact, predicts a slight strengthening of the jet. Actually, the model forecasts relatively little variation in the mean zonal wind profile from year to year compared with the observed wind analysis, and this is, of course, reflected in the behavior of the zonal kinetic energy, K_M, as noted earlier.

The relatively weak observed circulation over the Northern Hemisphere in January 1975 noted in Figs. 1 and 2, and indicated also by K_M in Table 1, appears to be due largely to a reduction of vertical wind shear in the upper troposphere over the sub-tropics. As shown by Wagner (1975), the zonal flow at 700 mb in January 1975 was actually "stronger than normal" over much of the Northern Hemisphere in middle and high latitudes, especially in the western hemisphere. Fig. 1 does, in fact, indicate that both observed and forecast westerlies were stronger than normal in the vicinity of latitude 50 N in January 1975. However, the observed sub-tropical wind maximum collapsed in 1975, and it is this latter feature that is poorly simulated in both the meridional and vertical forecast wind profiles. The possibility that the 1975 "observed" wind profiles and energetics in the Northern Hemisphere may not be correctly represented by the newly-adopted Flattery analysis at NMC cannot, of course, be discounted.

Interannual variations in the observed and predicted tropospheric mass fields are illustrated in Fig. 3, showing the mean meridional profiles of geopotential height at the 505-mb level, one of the nominal isobaric levels corresponding to the model's sigma-coordinate system. Again the general configuration of the mid-tropospheric isobaric surface is realistically simulated. The apparent discrepancies between forecast and observed heights in the Antarctic are probably due in part to the model's generation of an excessively warm Antarctic in summer and in part to a defect in the NMC analysis over that region. The anomalously high elevation of the isobaric surface observed in the Arctic in January 1974 is not predicted by the model, but otherwise the profiles are in good agreement.

As shown above, as well as in Somerville et al. (1974), the model does produce a realistic mean meridional structure for the month of January, although it fails to simulate realistically certain interannual variations of the zonally averaged global atmosphere. A more critical test of the model, however, would be of how well it reproduces the synoptic structure of the atmosphere as represented, for example, by the eddy energies. In Fig. 4 are shown the three January meridional profiles, for the Northern Hemisphere only, of the observed and predicted eddy kinetic energies averaged over pressure (height) and longitude. The units are 10^5 J m^{-2} bar^{-1}. As noted earlier, the eddy kinetic energy includes both transient and stationary eddies, so that this quantity reflects the temporal as well as spatial variability of the atmosphere within the month, and not merely the eddy structure of the mean maps.

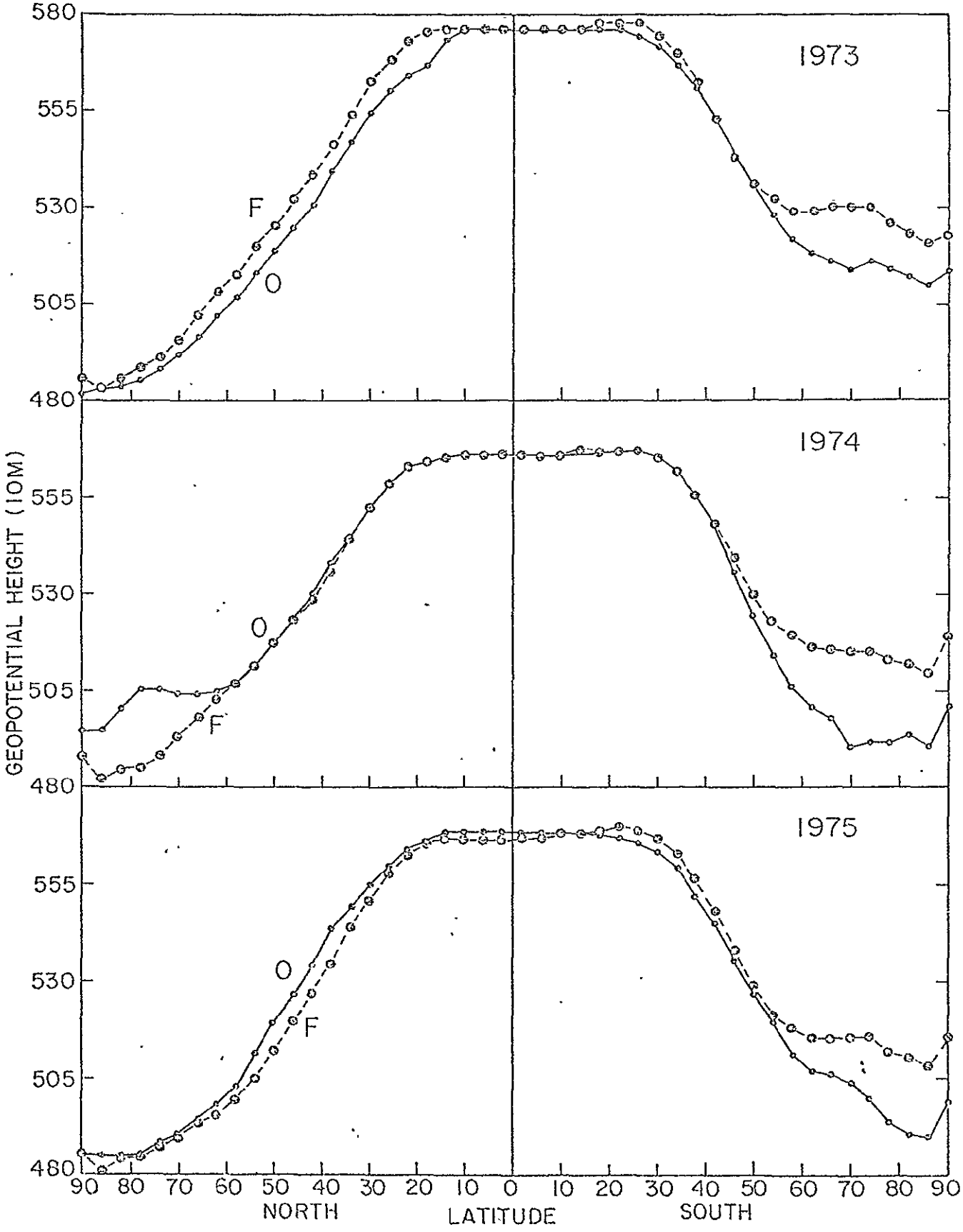
580
555
530
505
480
1973
F
O
1974
O
F
1975
O
F
GEOPOTENTIAL HEIGHT (10M)
90 80 70 60 50 40 30 20 10 0 10 20 30 40 50 60 70 80 90
NORTH
LATITUDE
SOUTH

FIG. 3

The interannual variations in eddy kinetic energy noted in Table 1 are now seen in more detail in the observed energy profiles (solid curves) in Fig. 4. January 1974 was the most active of the three months in terms of K_E (but not K_M), and a high K_E maximum is found in the 1974 profile in the vicinity of latitudes 45-50 N, about 10 degrees north of the maxima in the profiles for the other two years. (The 1974 profile is actually more similar to the 5-year K_E distribution of Peixoto and Oort (1974) than are the curves for 1973 and 1975.) However, the model fails to reproduce this peak in the energy profile, and indeed forecasts a higher mid-latitude maximum in 1973 than in 1974. In general, the model underpredicts the eddy kinetic energy in middle latitudes of the Northern Hemisphere each January. The discrepancy between observed and forecast eddy kinetic energies is most apparent in January 1975 when the model underpredicts the eddy kinetic energy everywhere in the Northern Hemisphere outside the tropics to yield the very low K_E minimum shown in Table 1. In the tropics, on the other hand, the model generates too much eddy kinetic energy each January compared with the observed atmosphere.

In summary, the model does not yet appear to be capable of accounting for the observed interannual variations in the mean meridional structure and circulation of the mean January atmosphere on the basis of the initial state of the atmosphere at the beginning of each month.

Error Statistics

The monthly mean forecasts have been evaluated in terms of rms errors and S1 skill scores (Teweles and Wobus, 1954), the latter being a dimensionless measure of the difference between predicted and observed horizontal gradients. (As in the case of rms errors, lower skill scores

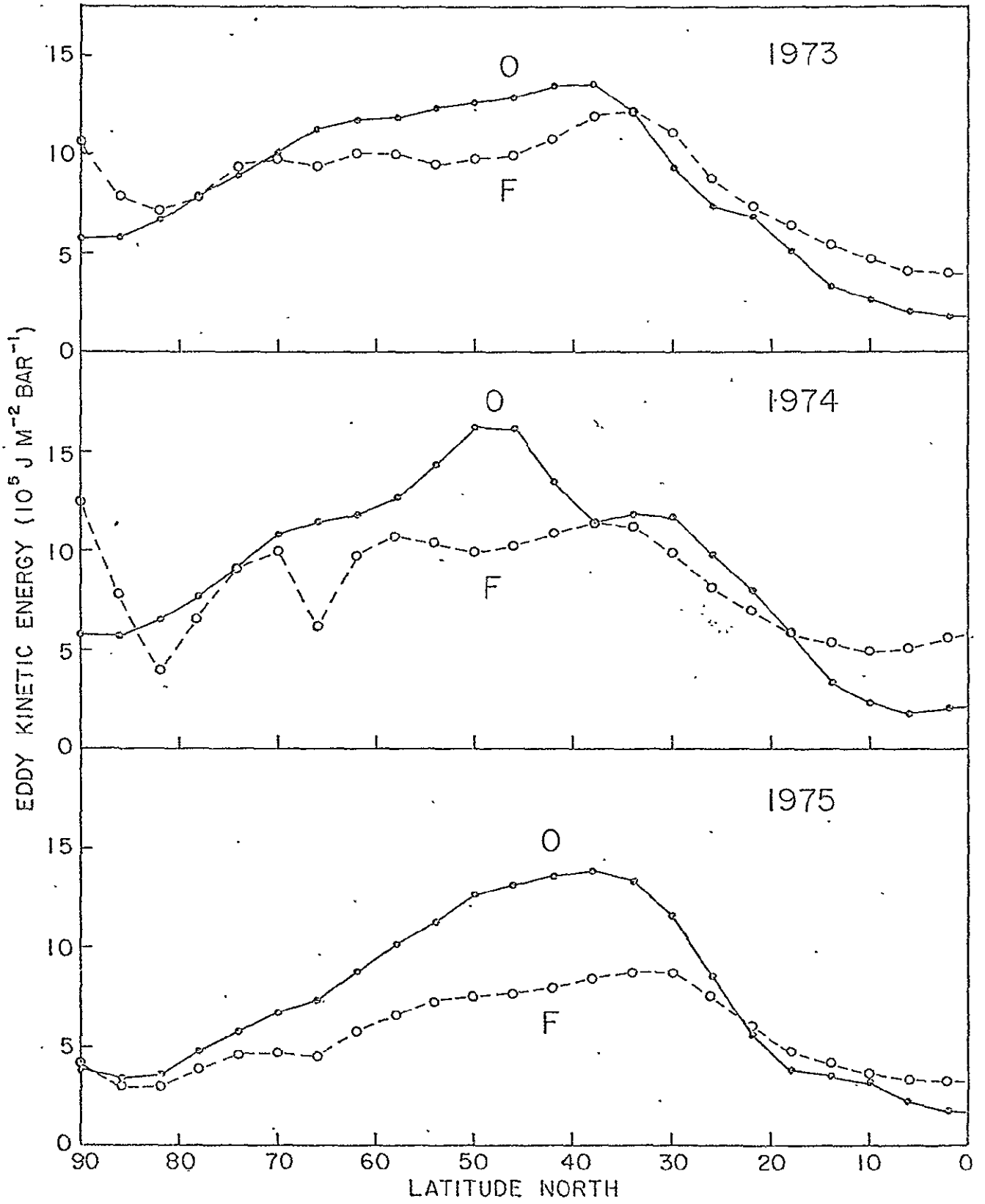
1973
1974
1975
O
F
EDDY KINETIC ENERGY (10^5 J M^{-2} BAR^{-1})
LATITUDE NORTH
0
5
10
15
90
80
70
60
50
40
30
20
10
0

FIG.4

signify better forecasts.) Both rms errors and S1 scores were computed for the sea-level pressure and 500-mb height fields, but only the rms errors were computed for the 850-mb temperature forecasts.

Verification statistics for each January forecast (F) are shown in Tables 3, 4, and 5 for seven different regions: the whole globe, the Northern Hemisphere, the tropical belt (22 N to 22 S), an eastern Pacific-United States region between latitudes 30-54 N and longitudes 75 W - 180,[13] North America between 30-70 N and 75-130 W, the United States between 30-54 N and 75-130 W, and a European region between 34-86 N and 10 W - 40 E. For the sea-level pressure and 500-mb height verifications, only land points were used in the North American, European, and United States verification regions.

For comparison, rms errors and S1 scores were also computed for two "no skill" forecasts represented by climatology (M) and persistence (P). (The global climatology "forecast" data for mean January were provided by the National Center for Atmospheric Research.) The persistence "forecast" for each January was taken to be the initial state of the atmosphere on 1 January (00 GMT) of that year.

In Tables 3, 4, and 5, the "best" forecast is underlined for each verification statistic, each forecast element, and each region. The model may be considered to be "successful" in a predictive sense only if it exceeds in skill both climatology and persistence. Of the 87 forecast verifications listed in the three tables, 53, or 61%, may be rated as "successful" by this criterion. Of course, the 87 forecasts are not independent. If they were, one could expect one-third to be "successful" just by chance on the assumption that F, M, and P are equally likely to excel, and one would have to concede some skill to the model. A more

[13] S1 scores were not computed for this region.

Table 3. (A) Root-mean-square (RMS) errors and (B) S1 skill scores of forecast (F) mean sea-level pressure (mb) for January 1973, 1974, and 1975. M and P denote climatology and persistence "forecasts", respectively. Minimum values are underlined.

A. RMS Error (mb)

Region	1973			1974			1975		
	F	M	P	F	M	P	F	M	P
Globe	8.5	10.9	9.2	7.6	7.6	9.2	6.0	5.9	5.5
Northern Hemisphere	10.0	8.7	12.2	8.6	9.2	11.7	6.1	6.6	7.2
Tropics	4.6	8.7	4.3	3.7	3.2	1.9	3.1	3.0	1.6
E. Pacific-U.S.	15.3	6.2	15.0	8.9	9.3	12.4	5.8	6.8	7.1
North America	12.8	7.1	12.5	4.7	5.5	10.8	7.2	10.0	12.4
United States	10.1	6.7	10.6	4.4	3.4	9.5	5.6	7.1	8.2
Europe	4.2	9.6	15.3	11.0	15.5	10.1	7.7	4.1	7.3

B. S1 Score

Region	1973			1974			1975		
	F	M	P	F	M	P	F	M	P
Globe	83	80	73	76	80	74	74	72	62
Northern Hemisphere	81	81	77	79	89	81	72	73	69
Tropics	77	75	68	71	80	60	71	67	50
North America	96	95	91	92	106	90	92	97	91
United States	97	98	89	92	101	97	95	103	85
Europe	73	87	69	84	110	95	77	55	76

Table 4. (A) Root-mean-square (RMS) errors and (B) S1 skill scores of forecast (F) mean 500-mb geopotential height (m) for January 1973, 1974, and 1975. M and P denote climatology and persistence "forecasts", respectively. Minimum values are underlined.

A. RMS Error (m)

Region	1973			1974			1975		
	F	M	P	F	M	P	F	M	P
Globe	<u>73</u>	97	89	<u>78</u>	88	93	64	68	<u>56</u>
Northern Hemisphere	<u>72</u>	94	119	<u>80</u>	108	116	<u>63</u>	82	73
Tropics	36	90	<u>35</u>	<u>15</u>	25	29	<u>19</u>	34	23
E. Pacific-U.S.	<u>85</u>	118	175	<u>68</u>	103	114	<u>84</u>	123	90
North America	<u>37</u>	132	146	84	<u>83</u>	151	<u>48</u>	130	117
United States	<u>36</u>	142	127	<u>79</u>	80	101	<u>49</u>	117	108
Europe	<u>40</u>	80	169	<u>98</u>	252	121	113	<u>38</u>	92

B. S1 Score

	1973			1974			1975		
	F	M	P	F	M	P	F	M	P
Globe	<u>50</u>	54	55	<u>51</u>	55	58	<u>43</u>	49	47
Northern Hemisphere	<u>45</u>	55	62	<u>53</u>	60	64	<u>42</u>	52	53
Tropics	<u>70</u>	73	<u>70</u>	<u>62</u>	72	69	<u>67</u>	71	58
North America	<u>34</u>	55	64	<u>38</u>	43	57	<u>34</u>	50	54
United States	<u>27</u>	48	65	<u>35</u>	41	52	<u>32</u>	40	50
Europe	<u>46</u>	58	69	<u>59</u>	84	79	53	<u>36</u>	68

Table 5. Root-mean-square errors of forecast (F) mean 850-mb temperature (deg. C) for January 1973, 1974, and 1975. M and P denote climatology and persistence "forecasts" respectively. Minimum values are underlined.

Region	1973			1974			1975		
	F	M	P	F	M	P	F	M	P
Northern Hemisphere	<u>4.1</u>	4.3	4.6	<u>4.7</u>	5.1	<u>4.7</u>	4.1	4.5	<u>3.6</u>
E. Pacific-U.S.	<u>4.3</u>	6.5	5.2	4.4	<u>3.3</u>	6.3	<u>4.9</u>	6.9	5.1
United States	<u>4.6</u>	7.8	5.4	4.6	<u>4.0</u>	7.8	<u>3.5</u>	7.5	5.2

interesting result, however, is revealed by considering separately the the 39 sea-level pressure, the 9 850-mb temperature, and the 39 500-mb height forecasts. For these three variables, the "successful" forecasts are found to total, respectively, 13 (33%), 6 (67%), and 34 (87%). Thus, it appears that, by this criterion, the model exhibits no skill over chance in forecasting monthly mean sea-level pressure, some skill in forecasting monthly mean 850-mb temperature, and considerable skill in forecasting the monthly mean 500-mb height field.

The average rms error of the three 500-mb height forecasts over the Northern Hemisphere (all "successful") is found to be 72 m for the model, compared with 95 m for climatology and 103 m for persistence. The average S1 skill score of the model at 500-mb over the Northern Hemisphere for the three January forecasts (all "successful") is 47, compared with 56 for climatology and 60 for persistence. The theoretical range of S1 skill scores extends from zero, for a perfect forecast, to a maximum of 200. However, National Weather Service forecasters consider an S1 score of 20 to be "virtually perfect" and a score of 70 to represent a "worthless" forecast (Shuman and Hovermale, 1968). Thus, as a measure of "percentage skill", the Weather Service frequently employs the quantity (70 - S1)/50. In terms of this quantity, the model's skill in predicting the monthly mean 500-mb height field over the Northern Hemisphere is thus 46%, compared with 28% for climatology and 20% for first day persistence. (It is noteworthy that, by the criterion above, none of the model's monthly mean sea-level pressure forecasts would be rated better than "worthless".)

The model's performance is particularly outstanding in the prediction of the 500-mb height field over the United States, where the mean rms error for the three Januarys is 55 m (compared with 113 m for climatology and 112 m for persistence), the mean S1 score is 31 (compared with 43 for climatology and 56 for persistence), and the mean percentage skill is 78% (compared with 54% for climatology and 28% for persistence.)

Prognostic and Observed Mean Maps

To illustrate the synoptic output of the model, maps of the mean predicted and observed sea-level pressure and 500-mb height fields are shown below for each January. Although global maps are presented, the analyses in the Southern Hemisphere are of rather dubious quality and the forecasts there are somewhat degraded by model deficiencies in the Antarctic. Therefore, in the interests of brevity, and in recognition of the uncertainties in the Southern Hemisphere, the discussion of the synoptic results in this section is limited to the Northern Hemisphere only.

Figs. 5, 6, and 7 display the global forecast and observed monthly mean sea-level pressure fields for each January, with isobars drawn for an interval of 4 mb. Figs. 8, 9, and 10 illustrate the corresponding 500-mb height fields, with geopotential height contours drawn for an interval of 100 meters. All fields have been slightly smoothed with a single 5-point smoothing pass.

In January 1973 the principal defects in the sea-level pressure prognosis (Fig. 5) for the Northern Hemisphere are found in the Aleutian and Icelandic regions, where the depths of the major mean cyclones are underpredicted. The model, in fact, generates an over-developed anticlone in the central North Pacific, extending from the subtropics to the Aleutian Islands, in place of the observed North Pacific low. On the

SEA LEVEL PRESSURE (MB-1000.)) SMOOTHED

FIG. 5(F)

SEA LEVEL PRESSURE (MB-1000.) SMOOTHED

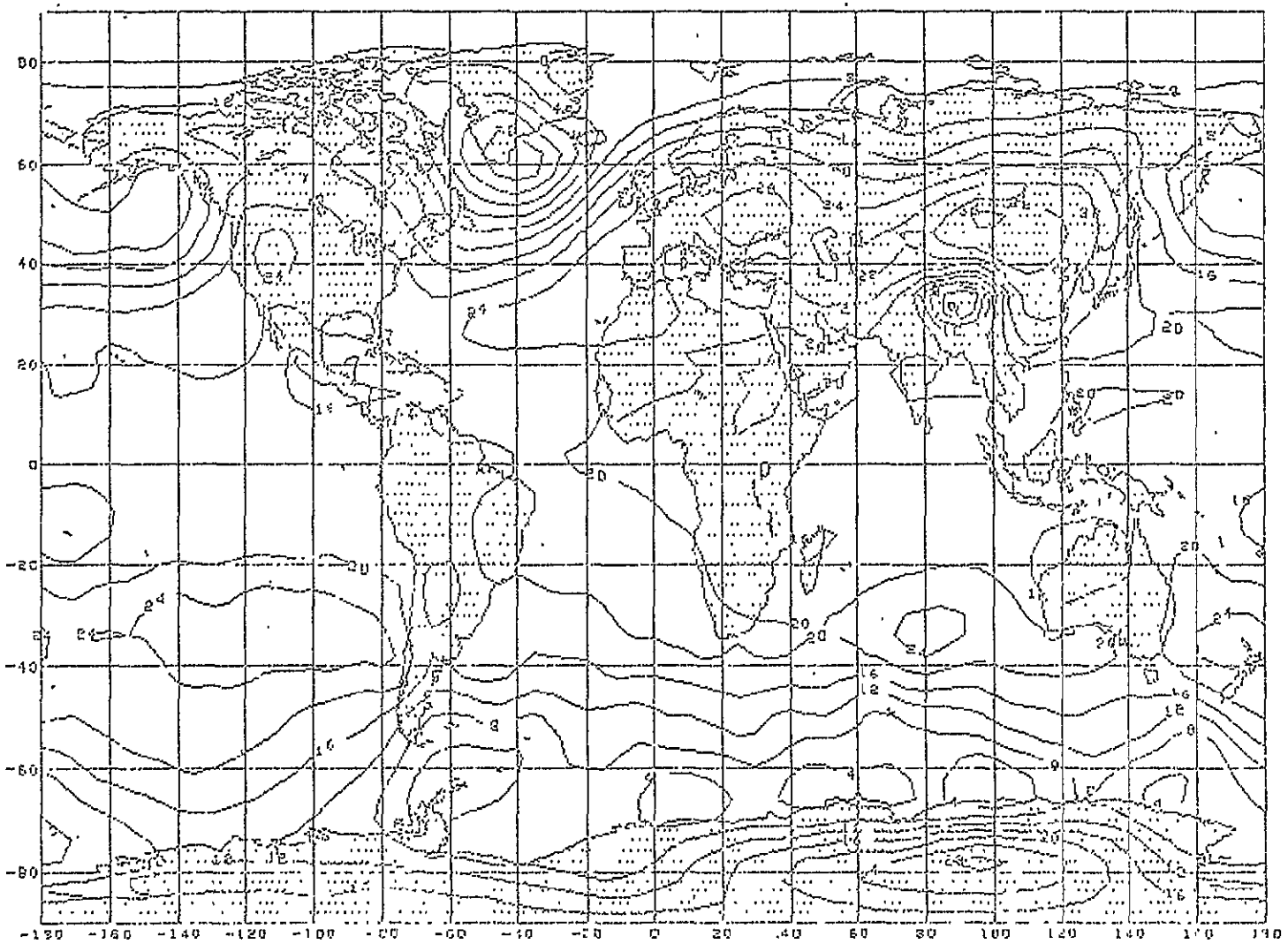

FIG. 5(O)

SEA LEVEL PRESSURE (MB-1000.)) SMOOTHED

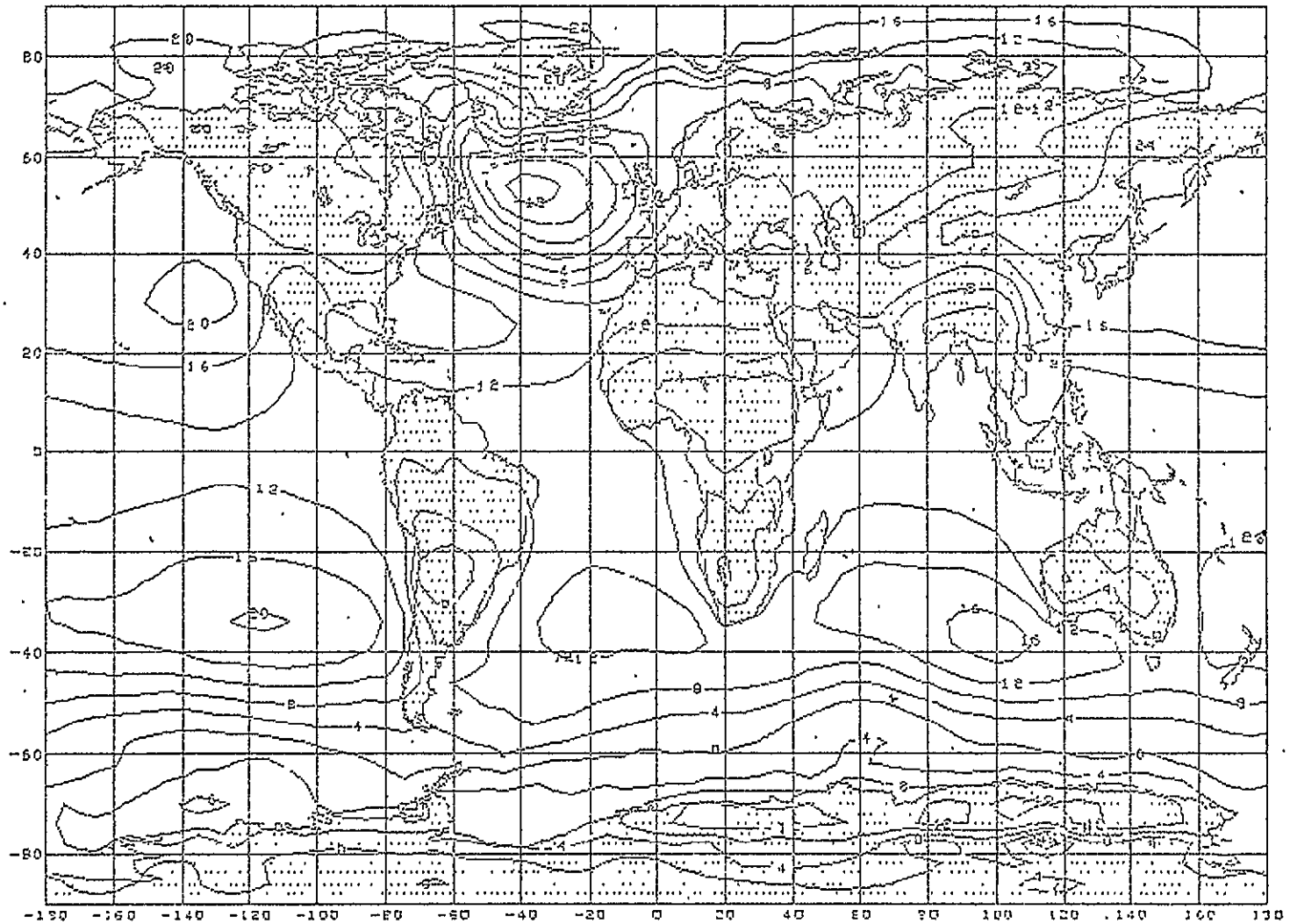

FIG. 6 (F)

SEA LEVEL PRESSURE (MB-1000.)) SMOOTHED

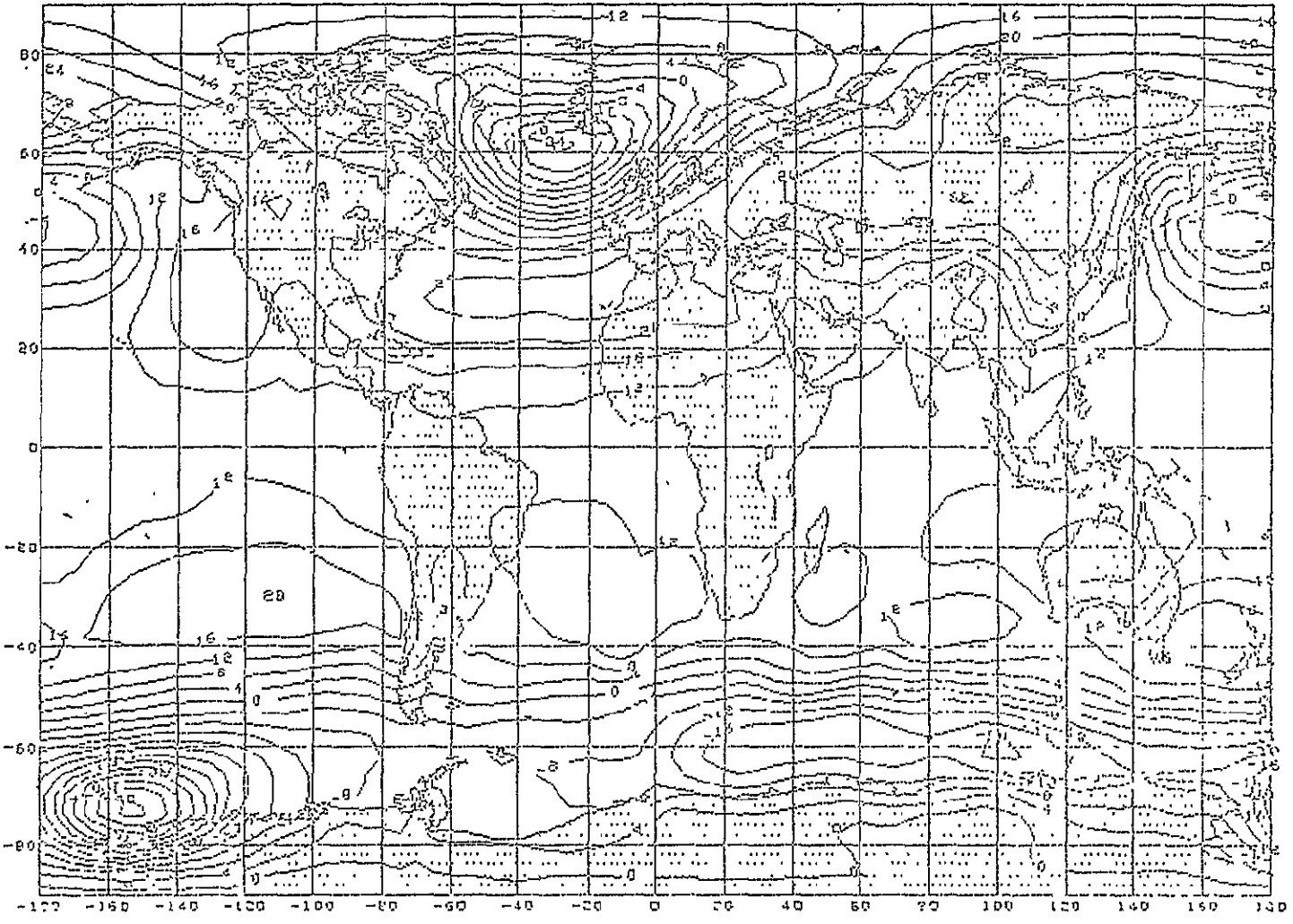

FIG. 6(O)

SEA LEVEL PRESSURE (MB-1000.)

SMOOTHED

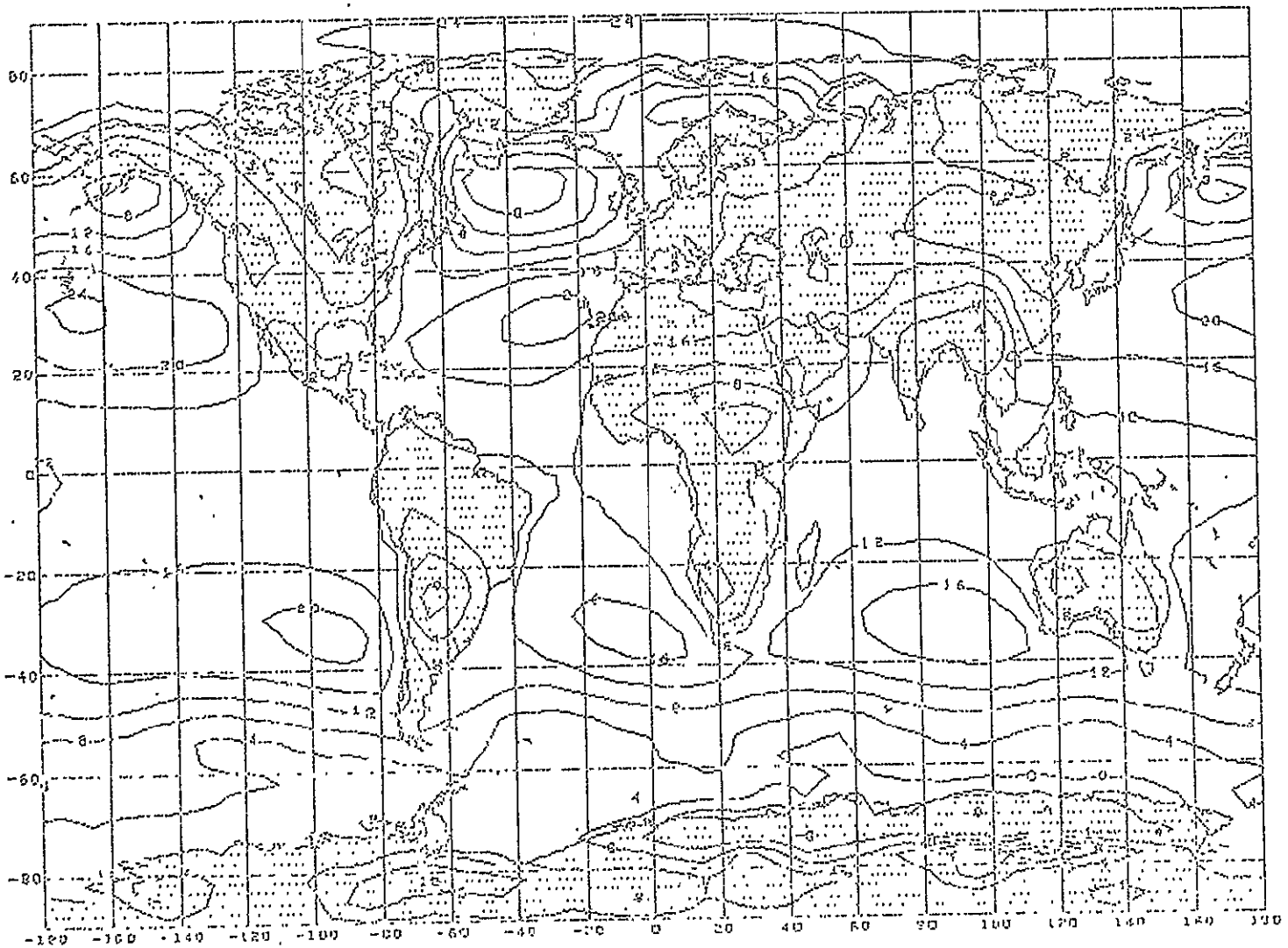

FIG. 7(F)

SEA LEVEL PRESSURE (MB-1000.)) · SMOOTHED

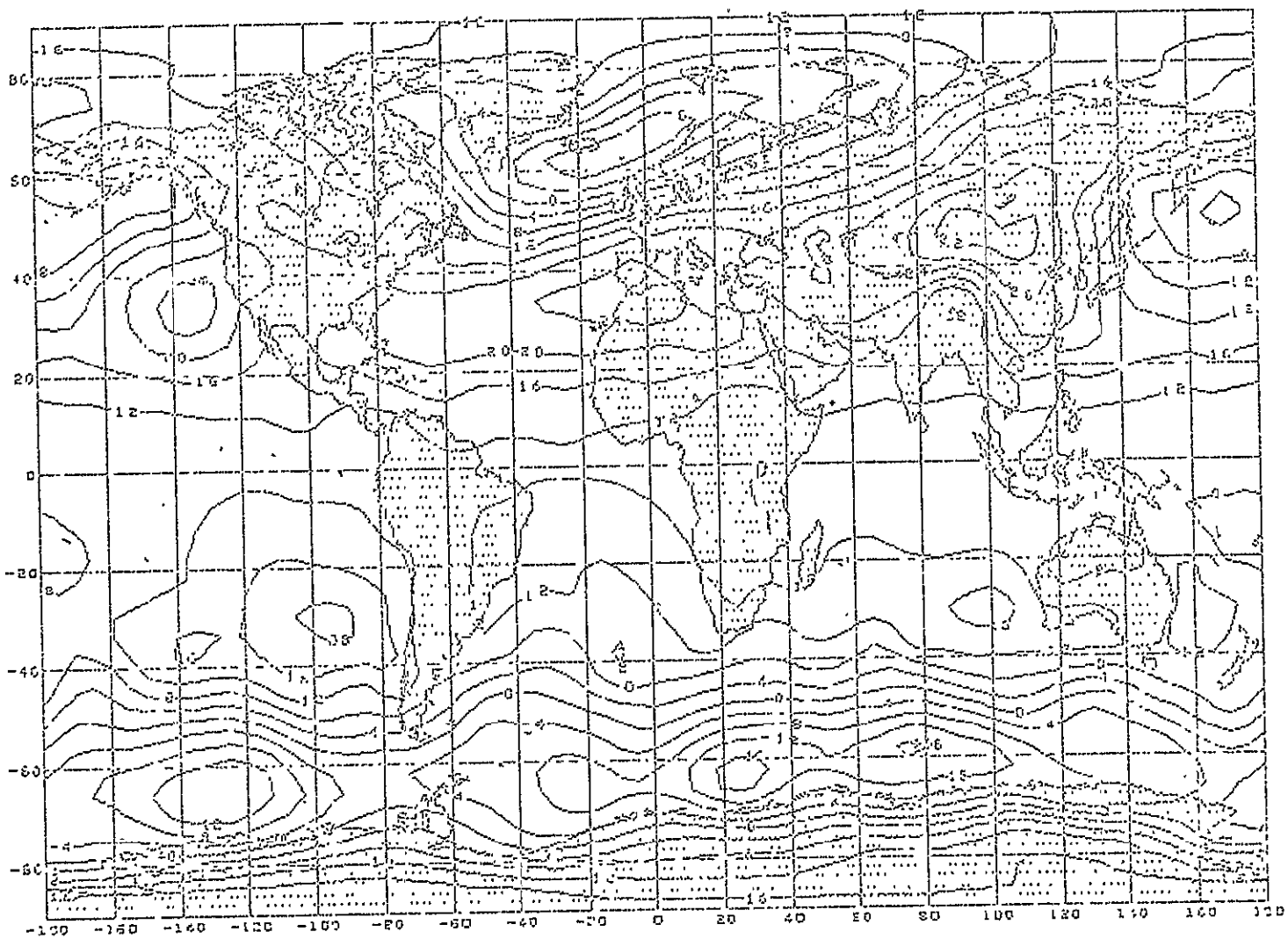

FIG. 7(O)

other hand, the North Atlantic pressure pattern is simulated fairly well, except for the cyclone depth, as is the Eurasian high pressure system. The prognostic map is generally unsatisfactory over the Northern Hemisphere, as indicated also by the poor error statistics for January 1973 shown in Table 3.

The prognostic sea-level pressure field for January 1974 (Fig. 6) is again mainly deficient in its simulations of the deep cyclone centers in the North Atlantic and North Pacific, particularly the latter, as well as the strong Siberian anticyclone. The predicted pressure field in the western North Pacific must again be rated as a failure, while that of the North Atlantic may be considered moderately successful, although neither the abnormal depth nor the location of the Icelandic low are accurately forecast. On the other hand, the troughs over Mexico and southeast Asia and the subtropical anticyclones are represented reasonably well by the model, and the North Atlantic cyclone is predicted (correctly) to be deeper than normal.

In January 1975 (Fig. 7), the model once again fails to predict correctly the location and depth of the low in the North Atlantic, as well as the Siberian anticyclone, on the mean sea-level pressure map. The result is a poor forecast of the pressure gradient over Europe. In the North Pacific the model predicts an overdeveloped subtropical high displaced too far to the west, and fails to account for the mean trough development in the central and western Pacific.

Despite the general inadequacy of the prognostic mean sea level pressure maps (reflected also in Table 3), the model does succeed in reproducing certain characteristics of the year-to-year variations in the mean January sea-level pressure field. The Icelandic low, for example

was observed to be relatively weak in 1973 and 1975 and very intense in 1974, with interannual changes in mean central pressure of about - 16 mb from 1973 to 1974 and +12 mb from 1974 to 1975. The forecast sea-level pressure maps indicate parallel interannual changes of about -20 mb from 1973 to 1974 and +12 mb from 1974 to 1975. Thus, while the model fails to predict the absolute magnitude of the pressure system in the North Atlantic, it appears to be capable of simulating an important interannual change in the mean January circulation pattern at sea level.

In contrast to the sea-level pressure fields, the monthly mean 500-mb height fields are predicted rather realistically by the model in all three months. Comparisons of the forecast and observed 500-mb contour patterns (Figs. 8, 9, 10) clearly illustrate what has already been shown in the error statistics of Table 4. Despite some obvious defects, such as phase shifts in the long waves, the agreement between forecast and observed fields is generally satisfactory. Furthermore, as indicated by Table 4, the model is not merely forecasting persistence or climatology, for, in terms of both rms errors and skill scores, the forecasts are superior to both climatology and persistence. The apparent skill of the model in the prediction of monthly mean 500-mb geopotential height fields is an encouraging result, which may have some practical value for long-range weather forecasting.

Of course, the 500-mb forecasts are not without serious defects. In January 1973 (Fig. 8), for example, the predicted wavelength over North America is too long, and the ridge forecast to lie over Alaska is actually found much farther east on the observed map. For January 1974 (Fig. 9) the strength of the northern hemisphere westerlies appears to be underpredicted. Furthermore, the 1974 westerlies are displaced too far south in the North Atlantic and too far north in the North Pacific on the pre-

GEOPOTENTIAL HEIGHT SURFACE 500 M B SMOOTHED

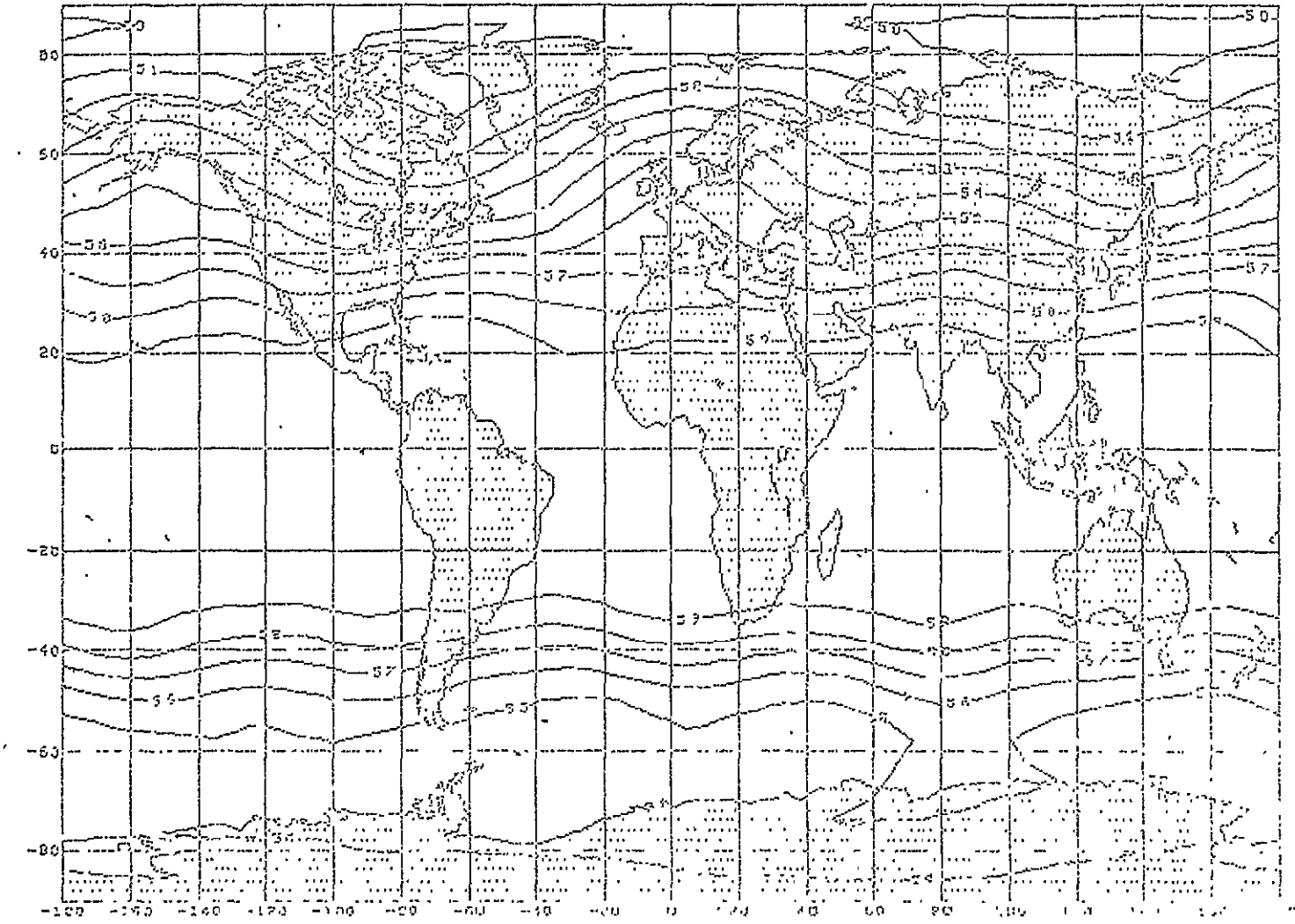

FIG. 8(F)

GEOPOTENTIAL HEIGHT SURFACE 500 M B SMOOTHED

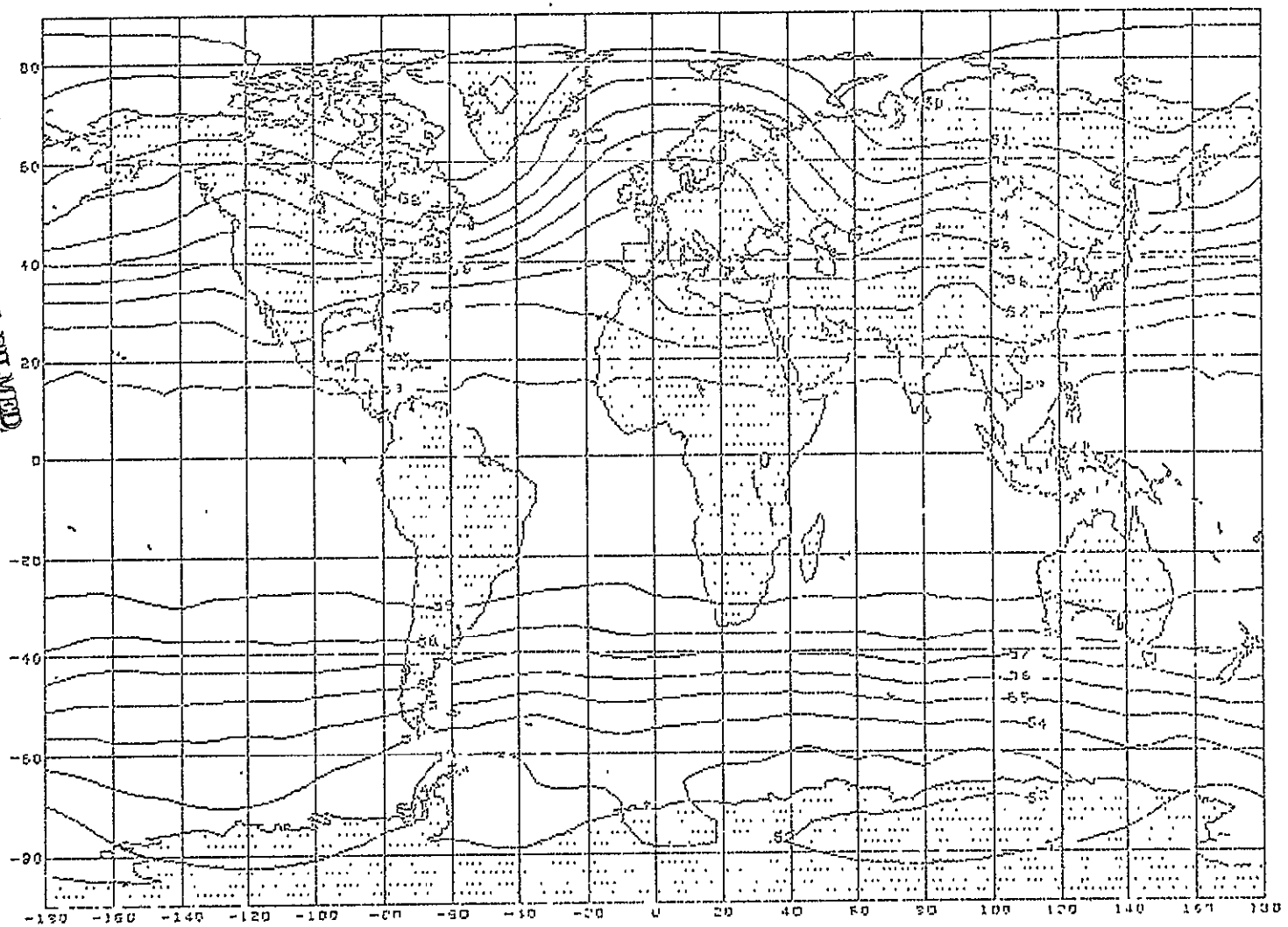

FIG. 8(O)

GEOPOTENTIAL HEIGHT SURFACE 500 M B SMOOTHED

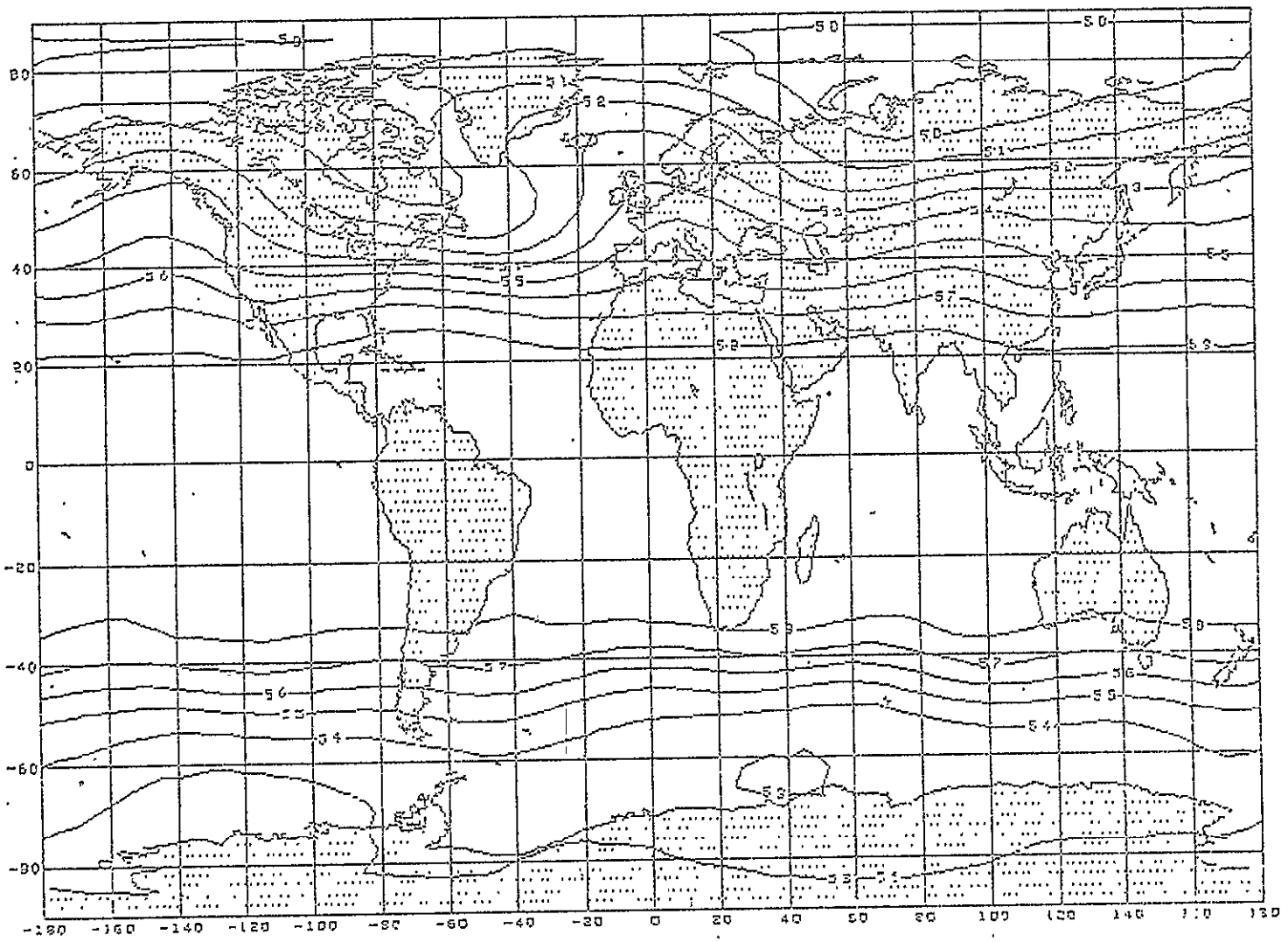

FIG. 9(F)

GEOPOTENTIAL HEIGHT SURFACE 500 M B UNSMOOTHED

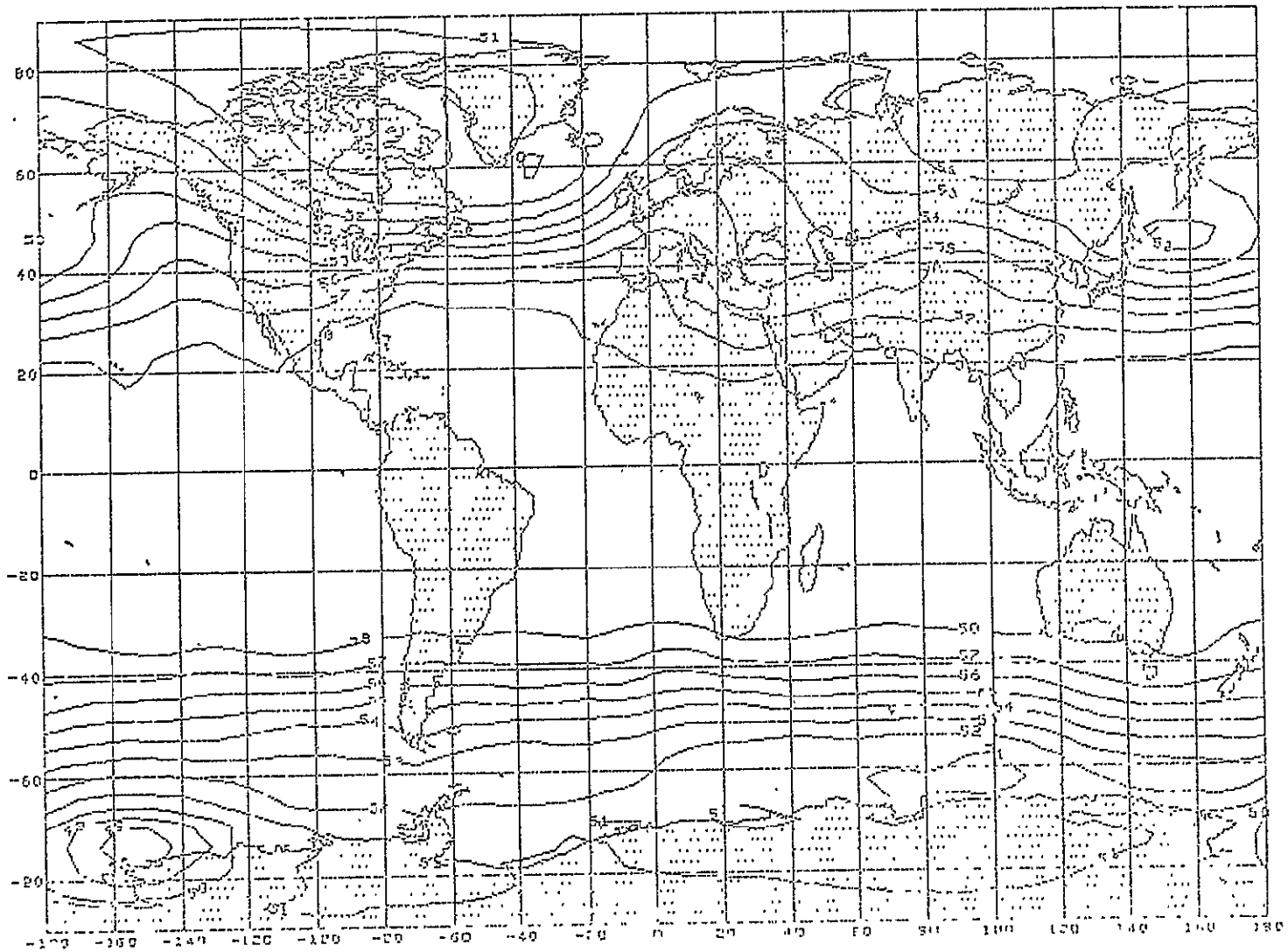

FIG. 9(O)

GEOPOTENTIAL HEIGHT SURFACE 500 M B SMOOTHED

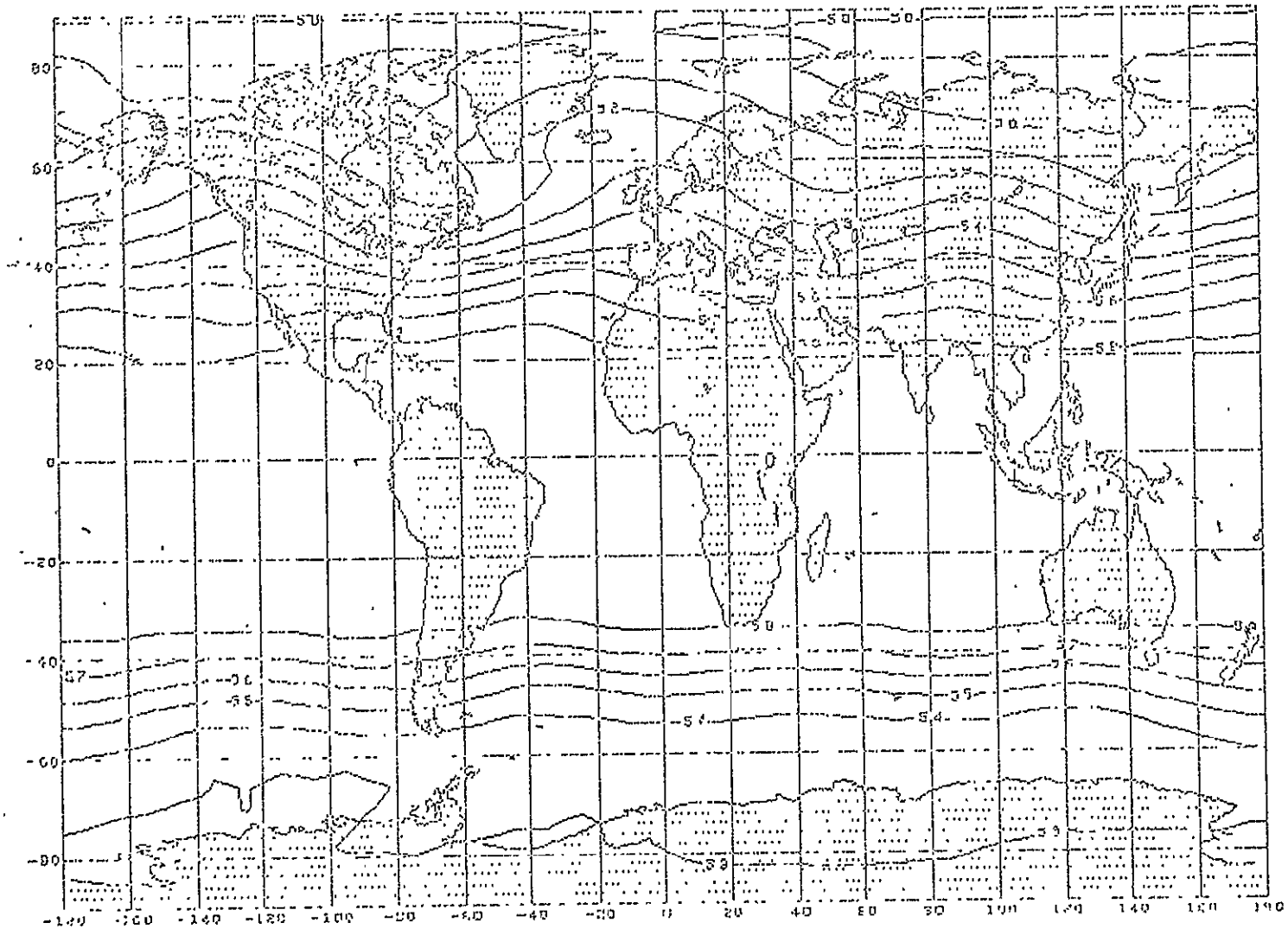

FIG. 10(F)

GEOPOTENTIAL HEIGHT SURFACE 500 M B UNSMOOTHED

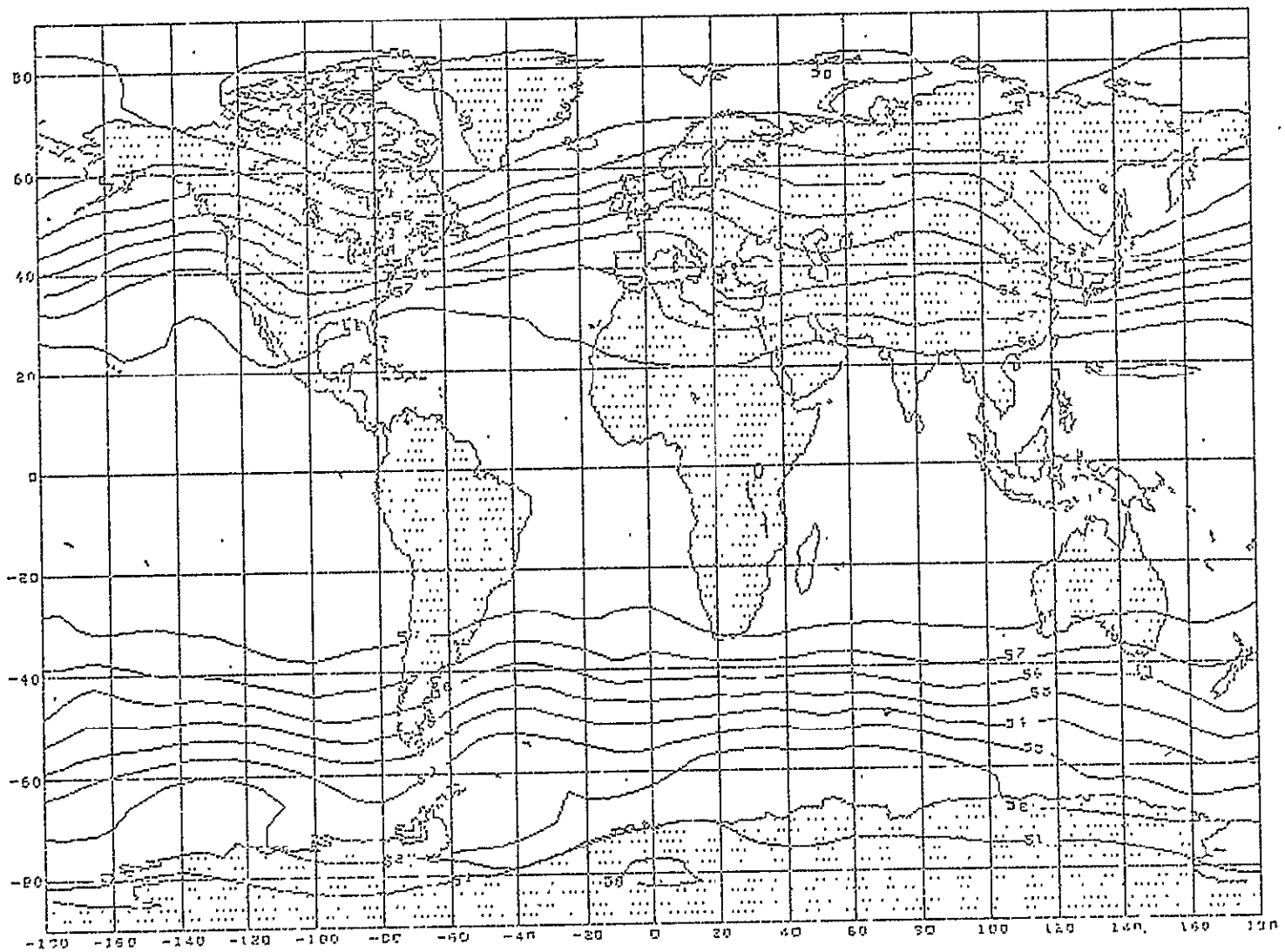

FIG. 10(O)

dicted map compared with the observed field, the amplitude of the predicted trough over the Black Sea region is too flat, and the closed circulation in the western Pacific is not predicted at all. On the other hand, the broad, flat, zonal current over the western hemisphere in January 1974, extending from the west coast of North America to the east coast of Europe, is simulated fairly well in the prognostic mean 500-mb map for 1974. The January 1975 500-mb forecast (Fig. 10) for the Northern Hemisphere is the most successful of the three in terms of both the error statistics in Table 4 and the synoptic mean maps. Phase agreement between the predicted and observed mean contours is good in middle latitudes, but less satisfactory in low and high latitudes. Major defects are found, however, north of Japan, where the trough amplitude is underpredicted, and east of Greenland, where the ridge amplitude is overpredicted.

In summary, the model generates a credible monthly mean prognostic map for the 500-mb level, and exhibits general predictive skill in excess of climatology and persistence, despite some obvious errors. At sea level the model is less successful, showing no general skill in forecasting the monthly mean sea-level pressure field, although it did succeed in reproducing the interannual changes in the depth of the mean January Icelandic low from 1973 to 1975.

3. SST UPDATE EXPERIMENT: January 1974

One of the many causes of forecast error in numerical weather prediction is incorrect specification of the sea-surface temperature (SST) field. Whether climatological or initial observed ocean temperatures are used for the calculation of surface fluxes over water, the SST field will eventually be in error unless it can be predicted. A successful coupled air-sea model may help to solve this problem. On the other hand, it is possible that an interactive model, through positive feedback of error, may have even worse predictability characteristics than one in which the SST field is constrained by climatology. Furthermore, even if a perfect SST forecast could be made, the influence of SST variations over the forecast period may prove to be negligible compared with other causes of decay of predictability (Spar and Atlas, 1975).

Some insight into the possibility of extending the useful range of atmospheric predictions by means of coupled models may be gained through experiments with a non-interactive atmospheric model in which the SST field, while prescribed, is altered during the forecast run to correspond to the observed ocean temperatures. In such an experiment, the atmospheric forecast is computed almost as it would be with a coupled model in which the ocean prediction provides a perfect SST forecast for the atmospheric calculations, but with the feedback simulated through the use of observed SST's.

In the GISS SST update experiment, two parallel forecasts were computed for January 1974 from initial data for 00 GMT, 1 January. For the Control (C) run the climatological January SST field was used for the entire month, while for the Anomaly (A) run the specfied SST values over the global ocean areas were updated at the beginning of each forecast day with the appropriate "observed" values at each gridpoint.

As noted earlier, The C forecast computed for January 1974 and described in this section os not quite the same as the January 1974 forecast (F) referred to in section 2 above, the latter having been run with an improved infrared radiation code and a geographically variable continental albedo. The F forecast computed with the "modified" model (see section 2) exhibits some marked improvements over the C forecast, notably a deeper and more realistic Icelandic low in the monthly mean sea-level pressure field, as well as some greater deficiencies, e.g., a weaker and less realistic Asiatic high pressure cell. In terms of rms errors and S1 skill scores, however, the original C forecast is actually somewhat better than the January 1974 F forecast made with the modified model over both the globe and Northern Hemisphere, although not over all sub-regions, as can be seen by comparing Tables 3-5 with Tables 7-9 below. For the purpose of assessing the impact of daily updated SST's on forecast quality, therefore, the original unmodified program was used to compute both the C and A forecasts described in this section.

Two sets of daily SST fields were used in the experiment. One set, obtained from the U.S. Navy Fleet Numerical Weather Central (FNWC), is derived from surface ship and buoy observations, supplemented by satellite data, and is available only for the Northern Hemisphere. The second set, derived from window channel infrared radiances monitored by meteorological satellite scanning radiometers, is available for the whole earth and was furnished by the National Environmental Satellite Service (NESS) of NOAA[14]. The two SST analyses are not entirely independent, as both use surface and satellite data, as well as climatological information, in the data processing. Nevertheless, the fields differ somewhat, and, as they complement each other geographically, both were used to derive a single global SST field for each day of the month.

---

14 National Oceanic and Atmospheric Administration.

The two fields were combined by a method designed to maximize the observed SST anomaly, i.e., the deviation from climatology, which in this case is the mean January SST. At the same time, excessive anomalies were viewed as being probably erroneous. In the Southern Hemisphere, NESS values were used exclusively. In the Northern Hemisphere, where both FNWC and NESS values were available, the value corresponding to the greater absolute anomaly was accepted. However, in both hemispheres, if the NESS value indicated an aboslute anomaly in excess of 6°C, it was discarded. If neither the FNWC nor NESS value was available at a grid-point, the January SST climatology was used.

In view of the well-known errors in sea-surface temperature measurements by ships (Saur, 1963), as well as the errors in SST's deduced from clear sky infrared radiances (Smith, et al., 1974; Wark, et al., 1974), it is probably not unreasonable to assign an uncertainty of ±1°C to both sets of values. Thus, daily SST anomalies smaller than ±1°C are almost certainly in the field noise and should be ignored. However, even larger anomalies are not necessarily reliable, particularly if they are of short duration and small scale, On the other hand, there are some persistent and larger scale features of the SST anomaly field which are more credible. These can be seen most clearly in the monthly mean SST anomaly fields for January 1974.

Three mean January 1974 SST anomaly maps are shown in Figs. 11, 12, and 13. Fig. 11 represents the global SST anomaly pattern based only on the "NESS" satellite data. Fig. 12 shows the SST anomaly pattern in the Northern Hemisphere derived from the FNWC data, and Fig. 13 illustrates the SST anomaly field resulting from the combination of NESS and FNWC data, which were used in the present experiment.

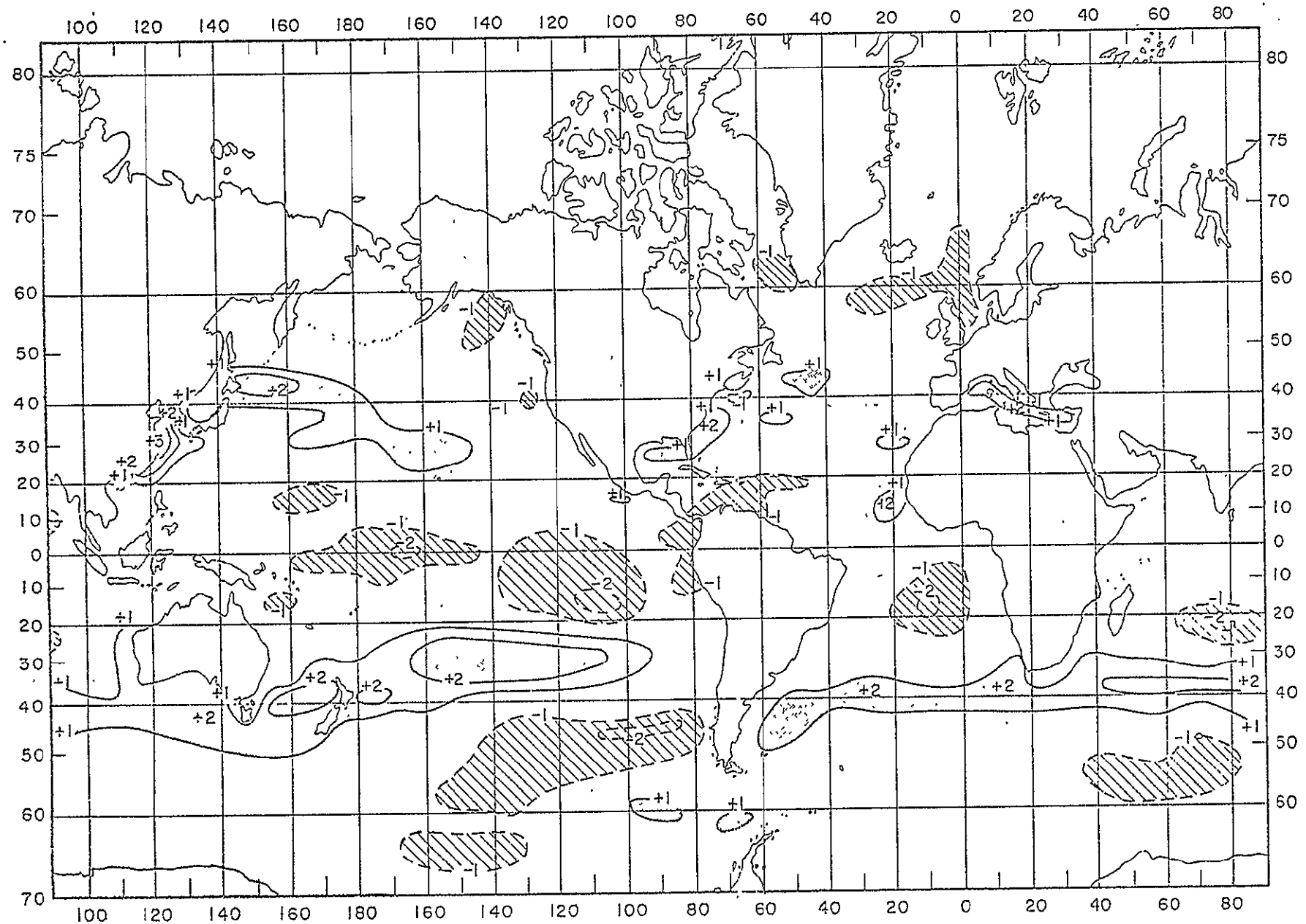
100 120 140 160 180 160 140 120 100 80 60 40 20 0 20 40 60 80
80 75 70 60 50 40 30 20 10 0 10 20 30 40 50 60 70

FIG. 11

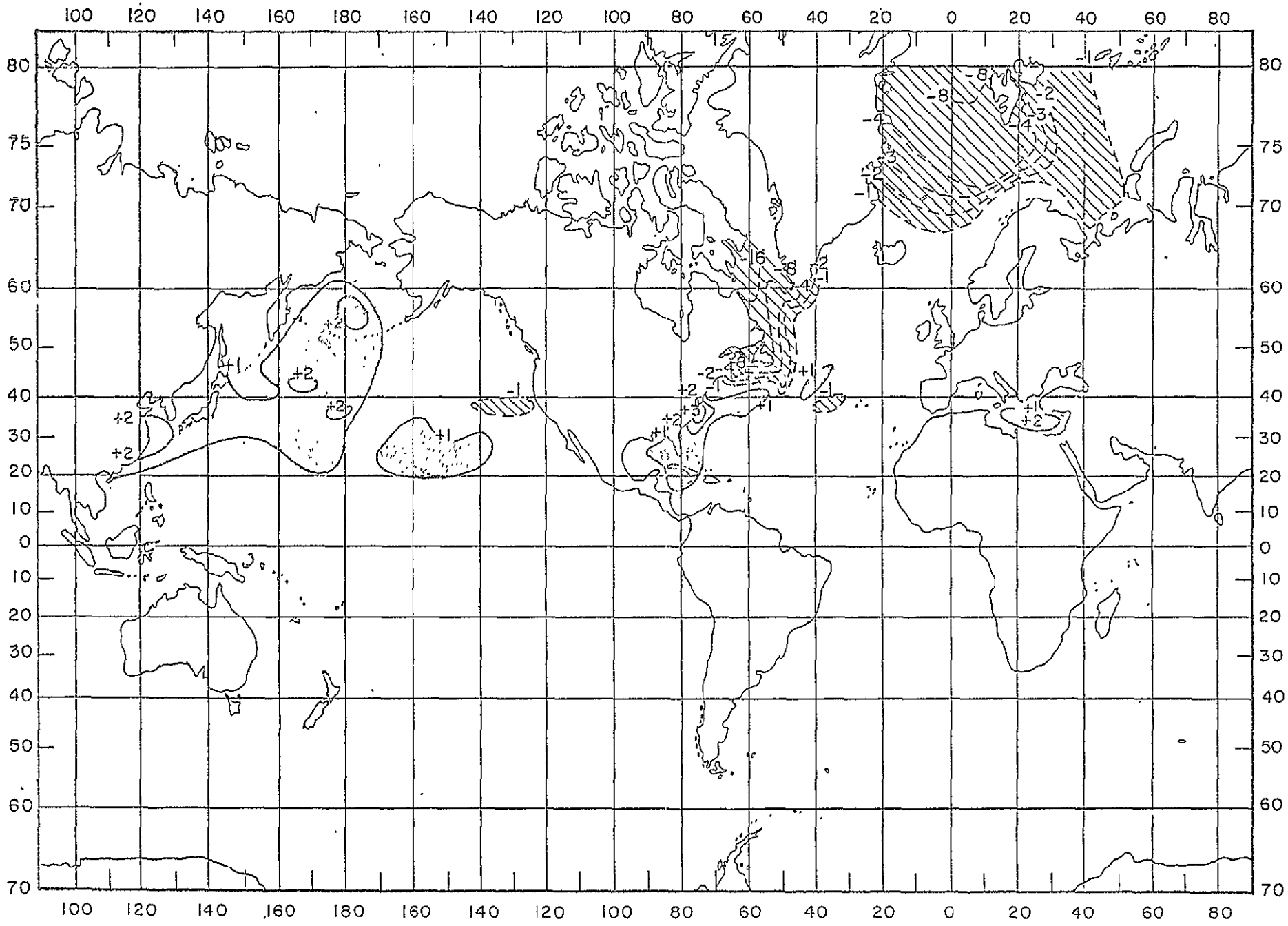
100 120 140 160 180 160 140 120 100 80 60 40 20 0 20 40 60 80
80 75 70 60 50 40 30 20 10 0 10 20 30 40 50 60 70
-8 -8 -1 -2 -3 -4 -1 -1
-16 -8 -4 -2 -1
-2 -4 -8 +1 +2 +3 +1 +2 +1 -1
+1 +2 +2 +2 +1 -1
+2 +2 +1 +2

FIG 12

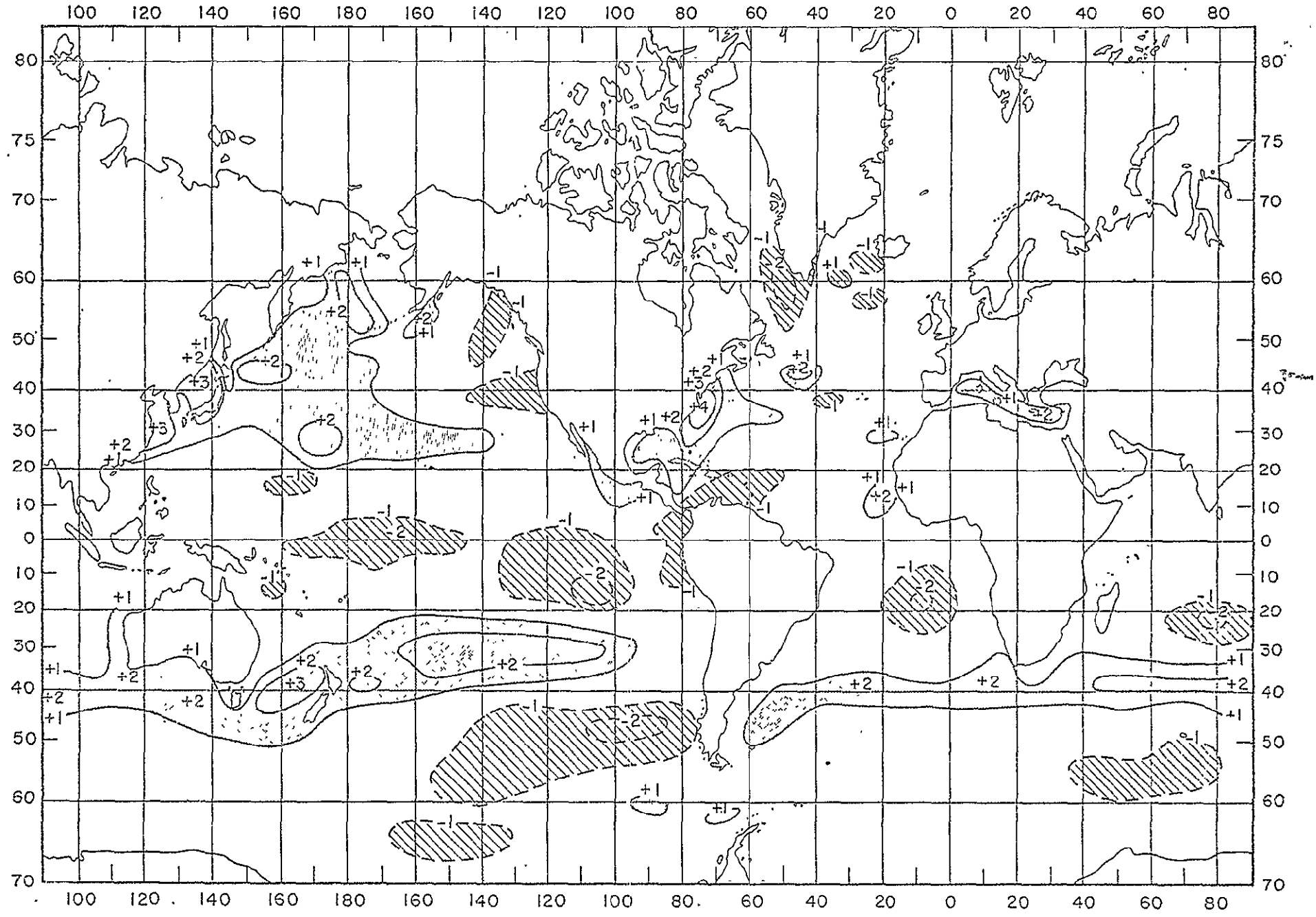
100 120 140 160 180 160 140 120 100 80 60 40 20 0 20 40 60 80
80 75 70 60 50 40 30 20 10 0 10 20 30 40 50 60 70

FIG. 13

In the Southern Hemisphere, where only NESS data (Fig. 11), were used, the SST anomaly field exhibits a banded zonal structure, with cold anomalies at low and high latitudes and warm anomalies in middle latitudes. The largest, and geographically most coherent SST anomalies are found in the South Pacific Ocean. The NESS SST anomaly field in the Northern Hemisphere Fig. 11) shows a similar general pattern of positive anomalies in middle latitudes, with negative anomalies in high and low latitudes, although it is not as well organized as in the Southern Hemisphere. The largest and most coherent warm anomalies in the Northern Hemisphere are found in the western Pacific, according to the NESS data (Fig. 11).

The mean January 1974 FNWC SST anomaly field (Fig. 12) is seen to be rather different from the NESS field in the Northern Hemisphere. Major differences between the two are found in high latitudes in both the Atlantic and Pacific Oceans, and off the east coast of North America. Near the Aleutian Islands and adjacent to the east coast of the United States, the FNWC field indicates warmer water than does the NESS field, while between Newfoundland and Greenland and north of Iceland the FNWC data show much colder water. Differences are also found off the west African coast, south of Iceland, in the mid-Atlantic, in the Gulf of Alaska, and in the sub-tropical Pacific. On the other hand, the principal warm SST anomalies on the western sides of the Atlantic and Pacific Oceans do appear on both maps.

The composite SST anomaly field (Fig. 13), resulting from the blending of the daily NESS and FNWC data for January 1974, is essentially the same as the NESS field in the Southern Hemisphere. In the Northern Hemisphere, on the other hand, the warm anomalies on the western sides of the oceans are (as might be expected from the blending method) larger both in magnitude and geographical extent on the composite map (Fig. 13)

than on the NESS map (Fig. 11). Thus, the composite SST anomalies, especially in the Pacific, exhibit even more clearly the zonal pattern of colder than normal sea temperatures in the equatorial region, and warmer than normal sea temperatures in middle latitudes of both hemispheres. (A possible consequence of this pattern of SST anomalies would be a weakening of both the thermally driven Hadley cell and the meridional transports by the tropical mean circulation (Bjerknes, 1966). The model did indeed generate such a response, but the effect was small and could not be verified against observations because of difficulties in estimating the observed mean meridional winds.)

Daily maps of SST anomalies for January 1974 (not shown) derived from NESS and FNWC data exhibit marked differences in the Northern Hemisphere. For example, large and persistent warm anomalies are found on the NESS maps in the western Atlantic and Pacific Oceans, off the east coasts of North America and Asia, and also in the Central Pacific. However, the east coastal anomalies on the daily FNWC maps are considerably smaller, weaker, and less persistent than those found in the NESS data, while in the central Pacific the warm anomaly is even larger and stronger in the FNWC data.

None of the anomalies persists for the full month without change; all parts of the anomaly field, whether in NESS or FNWC data, exhibit marked fluctuations during the month in both hemispheres. In the Southern Hemisphere, the anomaly field is initially irregular, small scale, and weak, then grows into a well-organized, broad-scale system towards the end of the month. In the Northern Hemisphere, on the other hand, initallly strong positive anomalies in the western Atlantic and in the western and central Pacific weaken during the month. Thus, the mean fields shown in Figs. 11, 12, and 13 do not represent constant features of the sea-surface temperature field during January 1974. The most consistent fea-

ture of the January 1974 SST anomaly field, one which is found almost every day in some form in both the FNWC and NESS data, is the anomalous warm water off the east coast of Asia.

One must, at this time, view the SST fields, particularly the daily patterns, with some skepticism. Both the observational methods and the techniques of analysis are imperfect, and there are undoubtedly real fluctuations in ocean temperatures on all scales which may or may not be represented in the course mesh data. It should also be noted that the month selected for this experiment was not characterized by unusually large and persistent SST anomalies, such as, for example, the 1968 anomaly studied by Namias (1971). Thus, we should be careful not to draw too general or sweeping conclusions regarding atmospheric response to sea temperature variations from this one experiment.

As expected, the daily forecast skill of the model degrades rapidly with time regardless of the SST field used. Fig. 14 illustrates the growth of rms errors in predicted sea-level pressure over the Northern Hemisphere at 24-hour intervals for a period of 3 weeks for both the C (dashed curve) and A (solid curve) forecasts. For the first 5 days the rms errors are virtually identical for the two forecasts. During the next 9 days the rms error of the A forecast is slightly smaller than that of the C forecast, but then it rises above the error of the C forecast during the third week. However, neither of the sea-level pressure forecasts retains any skill over climatology beyond 5 days, and the differences between the daily C and A forecast errors are clearly of no practical significance. Similar results (not shown) are found also at the 500-mb level over the Northern Hemisphere, although at that level both forecasts retain some skill over climatology up to about 10 days and the two sets of rms errors are almost identical for the three week period.

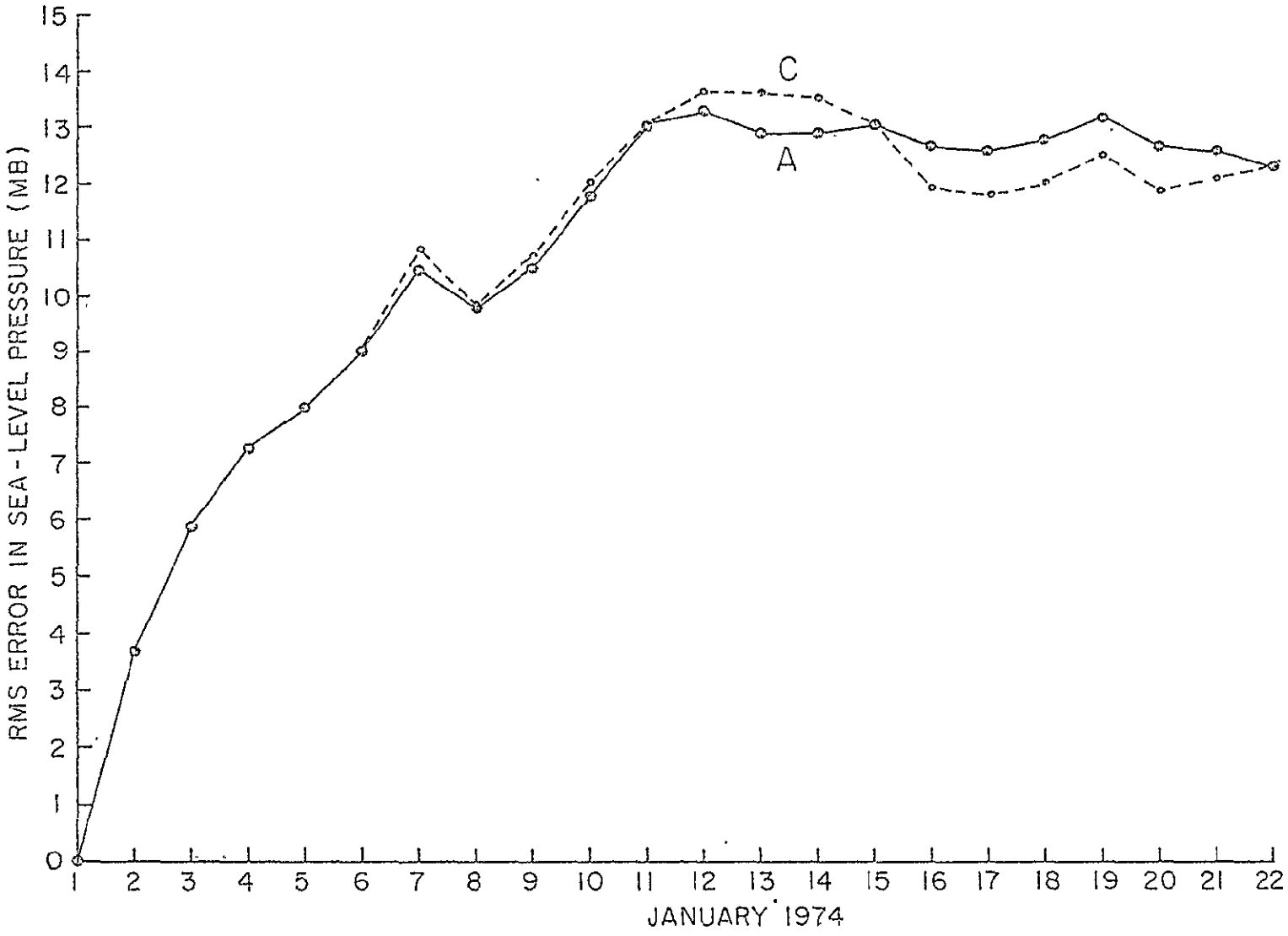
RMS ERROR IN SEA-LEVEL PRESSURE (MB)
0
1
2
3
4
5
6
7
8
9
10
11
12
13
14
15
C
A
1
2
3
4
5
6
7
8
9
10
11
12
13
14
15
16
17
18
19
20
21
22
JANUARY 1974

FIG.14

These results are consistent with those of Spar and Atlas (1975) who found that the use of observed SST values did not yield any detectable improvement in the quality of daily large-scale prognostic maps over a two-week period.

The monthly mean sea-level pressure fields for January 1974 forecast with either the C or A model suffer from certain obvious defects as seen in Fig. 15 for the Northern Hemisphere. In the North Atlantic, the predicted Azores - Bermuda high and Icelandic low are too weak compared with the observed systems. Hence, the predicted pressure gradients in the North Atlantic are also much weaker than observed. In the North Pacific, the forecast Aleutian low is not only weaker than observed, but is displaced too far to the east, so that again the predicted pressure gradient in the western Pacific is much weaker than observed, and the pressure field is, in fact, quite unrealistic.

Comparing the A and C forecasts, one finds only a relatively small, and indeed negative, influence of the SST anomalies on the predicted mean monthly sea-level pressure field. The Icelandic low and Azores - Bermuda high are both slightly weaker in the A than in the C forecast, and, hence, the predicted sea-level pressure gradients in the North Atlantic are even more in error in A than in C. The deep cyclone in the western Pacific is not well predicted in the A computation, being displaced into the eastern Pacific, resulting in an even less satisfactory sea-level pressure field than that forecast by C. However, the difference (not shown) between the C and A forecast mean sea-level pressure fields are so small that they are undoubtedly well below the noise level of the model, and are of no practical significance. (For a study of the noise level of a general circulation model, specifically the NCAR model, see Chervin and Schneider (1975 a,b).) Although corresponding noise level maps based on multiple random perturbations of the initial state are not yet available for the GISS model, it is reasonable to expect that they would resemble those computed for the NCAR model.)

SEA LEVEL PRESSURE (MB-1000.) SMOOTHED

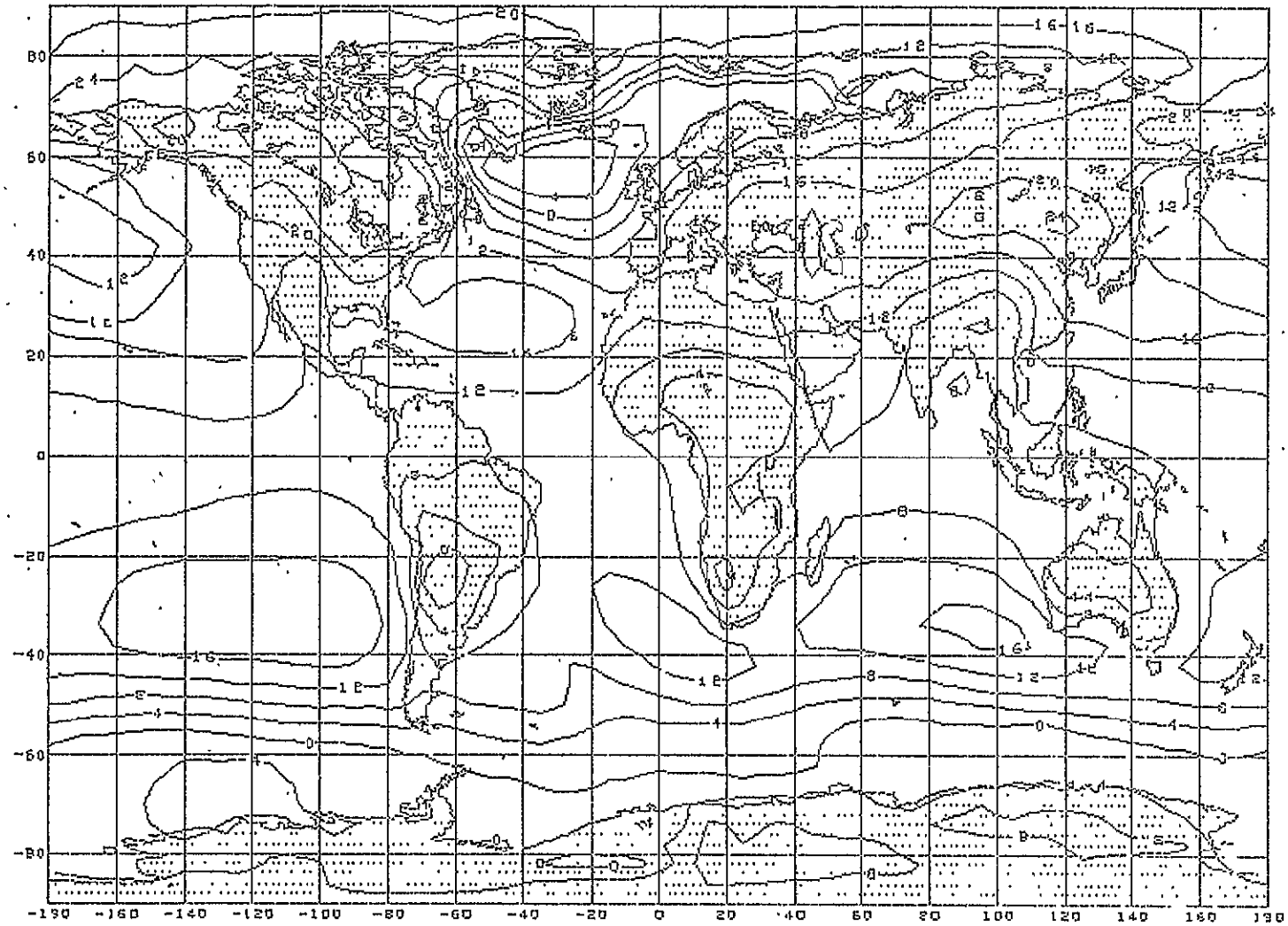

FIG. 15(C)

SEA LEVEL PRESSURE (MB-1000.)) SMOOTHED

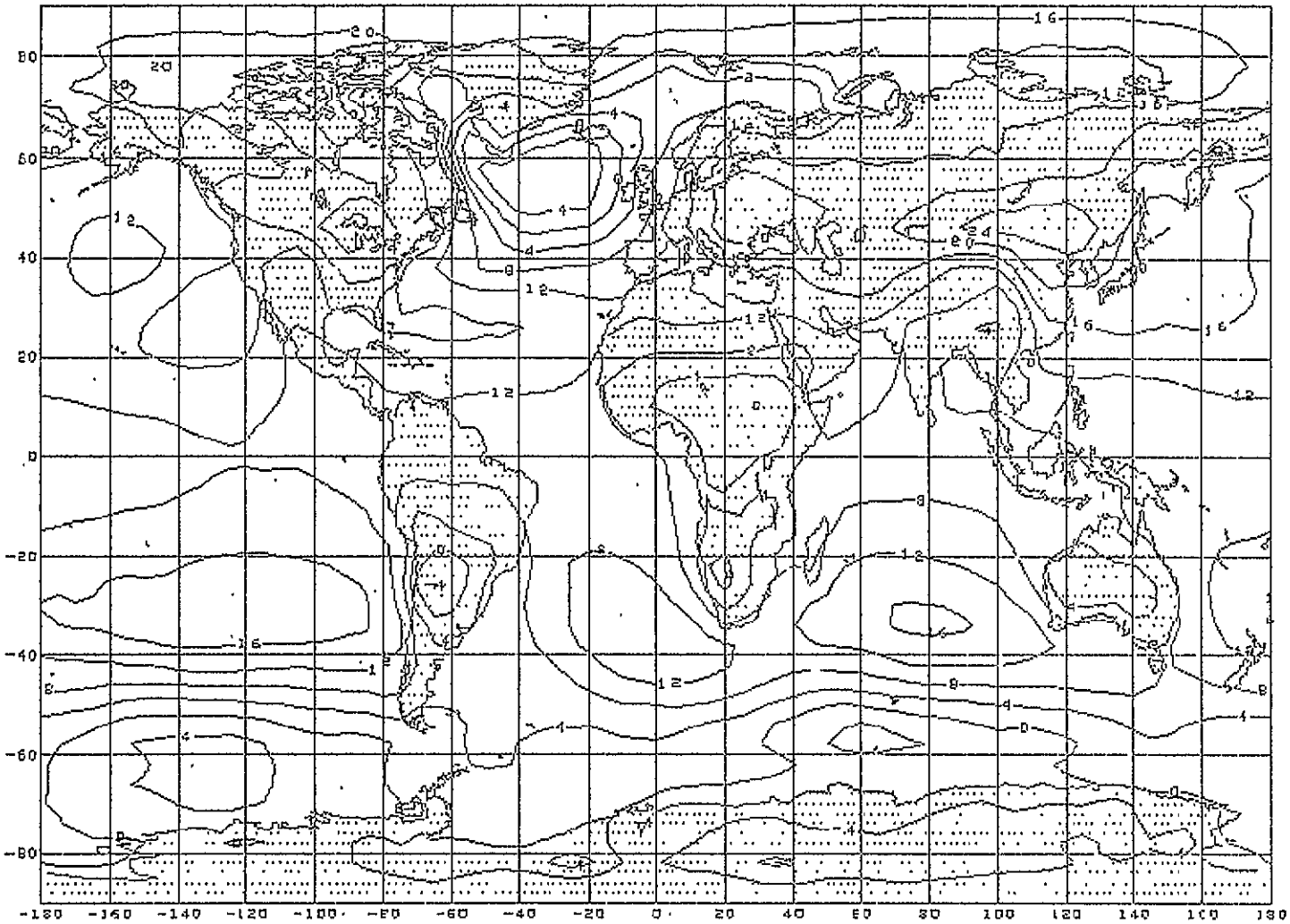

FIG. 15 (A)

SEA LEVEL PRESSURE (MB-1000.0)

SMOOTHED

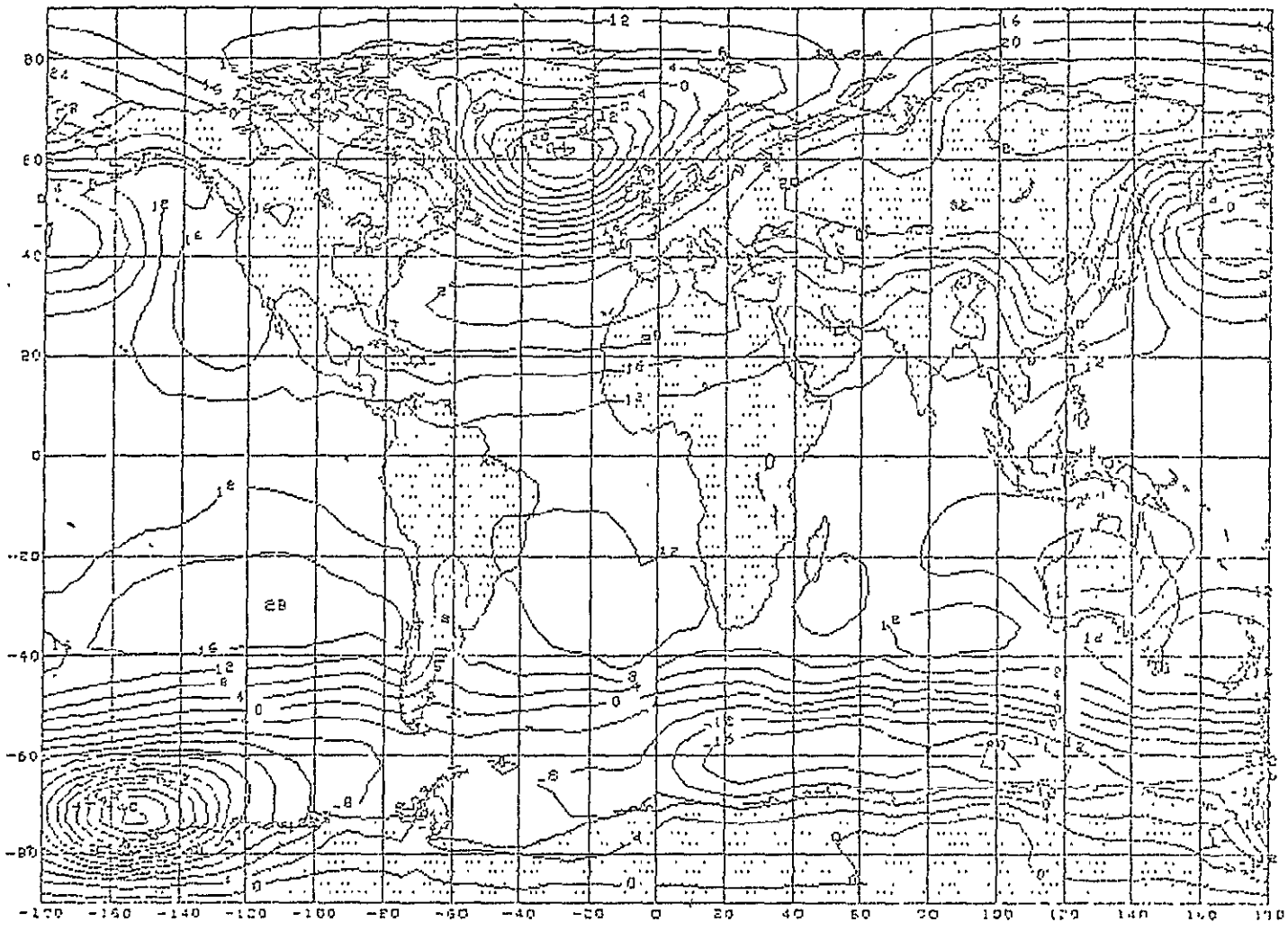

FIG. 15(O)

Another qualitative test of the impact of a variable SST field on forecast skill is the degree to which the deviation of the atmosphere from its climatological normal state is predicted. In particular, it is of interest to know how the major "centers of action" in the sea-level pressure field in a given month depart from normal, and whether these departures are better predicted by a forecast computed with a variable SST field than by one based on climatological SST's. In Table 6 are listed the latitudes, longitudes and central pressures of the five major sea-level pressure systems in the Northern Hemisphere, including the normal January positions and pressures (estimated from Crutcher and Meserve, 1970), the observed January 1974 values, the values predicted by the C and A runs, and, for comparison, the values for January 1973. Although they are of no particular statistical significance, the data shown in Table 6 do indicate the relative impact of the SST anomalies on the monthly mean forecast sea-level pressures.

The Icelandic low was much deeper than normal on 1974, but close to its normal position. Both its location and the sign of its sea-level pressure deviation from normal were, in fact, correctly predicted by the C forecast, although the depth of the Icelandic low was not. The A forecast, on the other hand, did not improve on the C forecast either in location or central pressure. The subtropical Atlantic high pressure belt was also close to its normal pressure and latitude in January 1974. While both the C and A computations indicated approximately the correct latitude for the system, neither forecast the pressure correctly, and, of the two, the A forecast was the poorer with regard to the deviation from normal. The continental anticyclone over Siberia in January 1974 was in a nearly normal state of development, but split into two centers.

Table 6. Locations and central pressures of the major centers of action in the Northern Hemisphere

System		Normal January	Observed January 1974	C-Forecast	A-Forecast	January 1973
Icelandic Low	Lat.	60N	60N	59N	55N	60N
	Long.	30W	30W	30W	30W	40W
	Pressure (mb)	996	974	992	994	986
Azores Bermuda High	Lat.	25 - 35N	30N	28N	28N	25 - 35N
	Long.	-	-	-	-	-
	Pressure	1024	1025	1018	1016	1024
Asiatic High	Lat.	50N	50N + 65N	45N	45N	45N
	Long.	95E	95E	120E	120E	110E
	Pressure	1034	1032	1024	1024	1030
Pacific Low	Lat.	50N	45N	45N	40N	55N
	Long.	165W + 170E	170E	180	160W	145W + 170E
	Pressure	998	994	1010	1010	1002
East Pacific High	Lat.	30N	30N	30N	30N	28N
	Long.	140W	130W	130W	130W	130W
	Pressure	1022	1018	1018	1018	1022

Both forecasts placed the high center east of its observed (and normal) position, and both were equally in error in the central pressure. In the Pacific Ocean, the western lobe of the Aleutian low was dominant in January 1974, and slightly deeper than normal. Both foreaasts failed to reflect this development, indicating a weaker than normal Aleutian low, displaced too far to the east, with the larger position error in the A forecast. The east Pacific high pressure cell on the other hand was equally well-predicted by both the C and A runs. Thus, in a subjective, qualitative sense, the use of daily updated SST's did not improve the prognostic monthly mean sea-level pressure field for January 1974.

The forecast mean 500-mb height fields for January 1974 with and without SST updating are illustrated in Fig. 16. As in the case of the sea-level pressure fields, the differences between the C (top) and A (middle) forecast fields are relatively small compared with the differences between either of the forecasts and the "observed" (bottom) field. Both the C and A forecasts are about equally satisfactory in the western hemisphere and about equally unsatisfactory in the western North Pacific. (Compare also the forecast and observed 500-mb fields in Fig. 9.) Thus, again in a subjective, qualitative sense, the use of daily updated SST's did not improve the prognostic monthly mean 500-mb height field for January 1974.

A more quantitative demonstration of the impact of the updated SST's on forecast quality is presented in Tables 7-9, showing the rms errors and S1 skill scores, respectively, for sea-level pressure, 500-mb height, and 850-mb temperature (rms error only) for both the control (C) and anomaly (A) forecasts. Also shown again for comparison are the climatology (M) and persistence (P) forecast scores, as in Tables 3-5. The geographical regions are the same as in Tables 3-5, and minimum values are again underlined.

GEOPOTENTIAL HEIGHT SURFACE 500 M B SMOOTHED

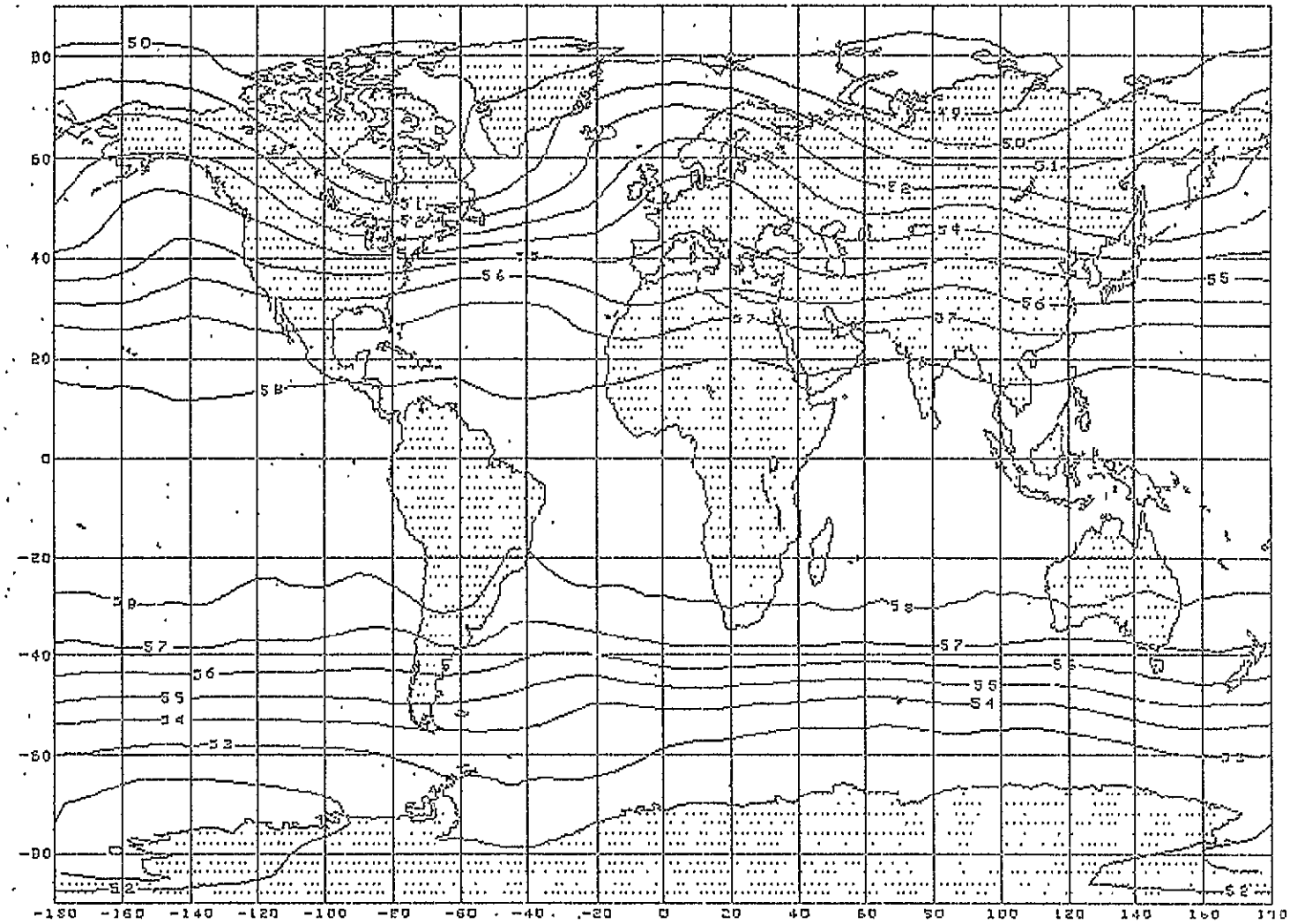

FIG. 16(C)

GEOPOTENTIAL HEIGHT SURFACE 500 M B SMOOTHED

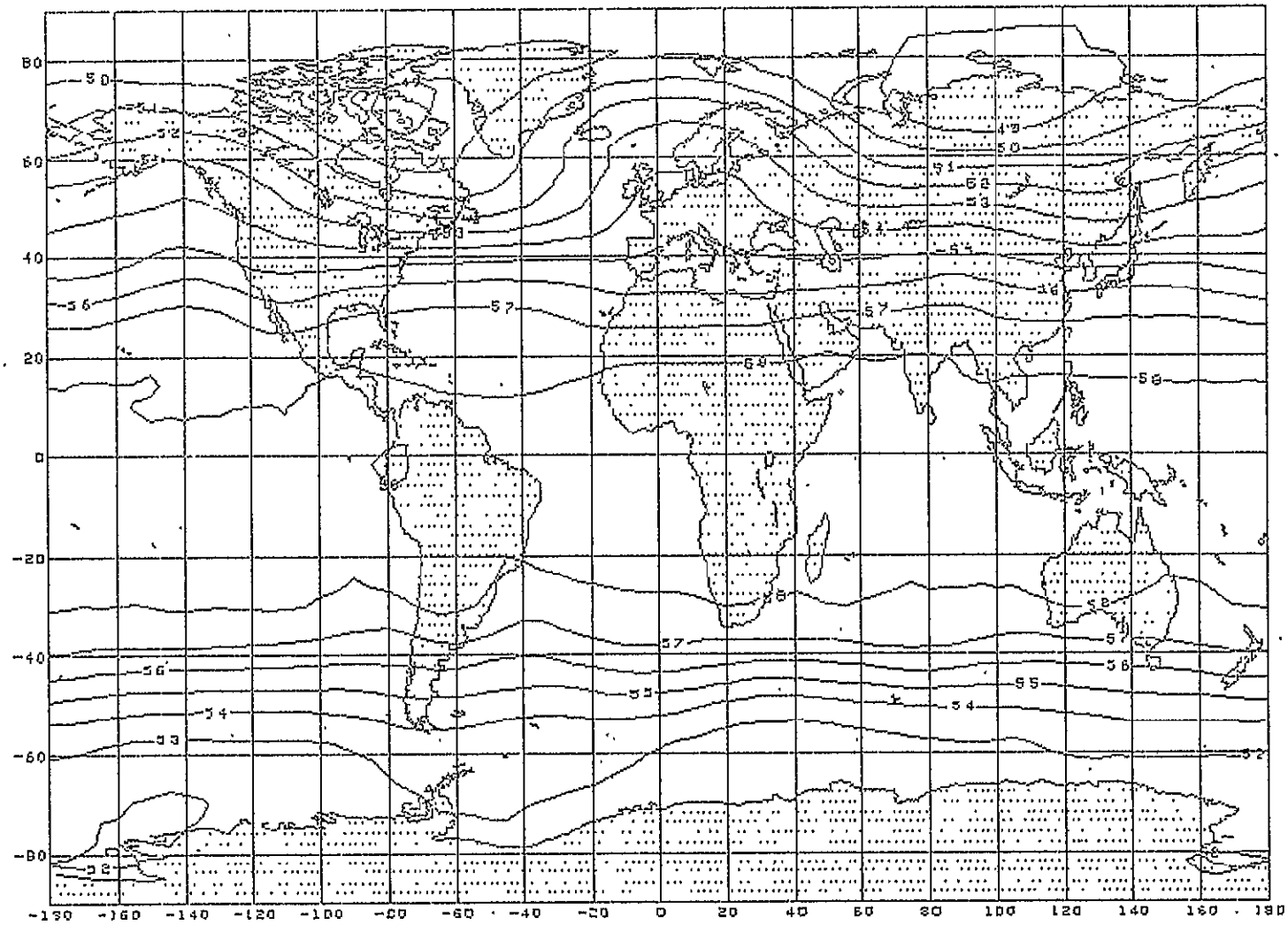

FIG. 16(A)

GEOPOTENTIAL HEIGHT SURFACE 500 M B UNSMOOTHED

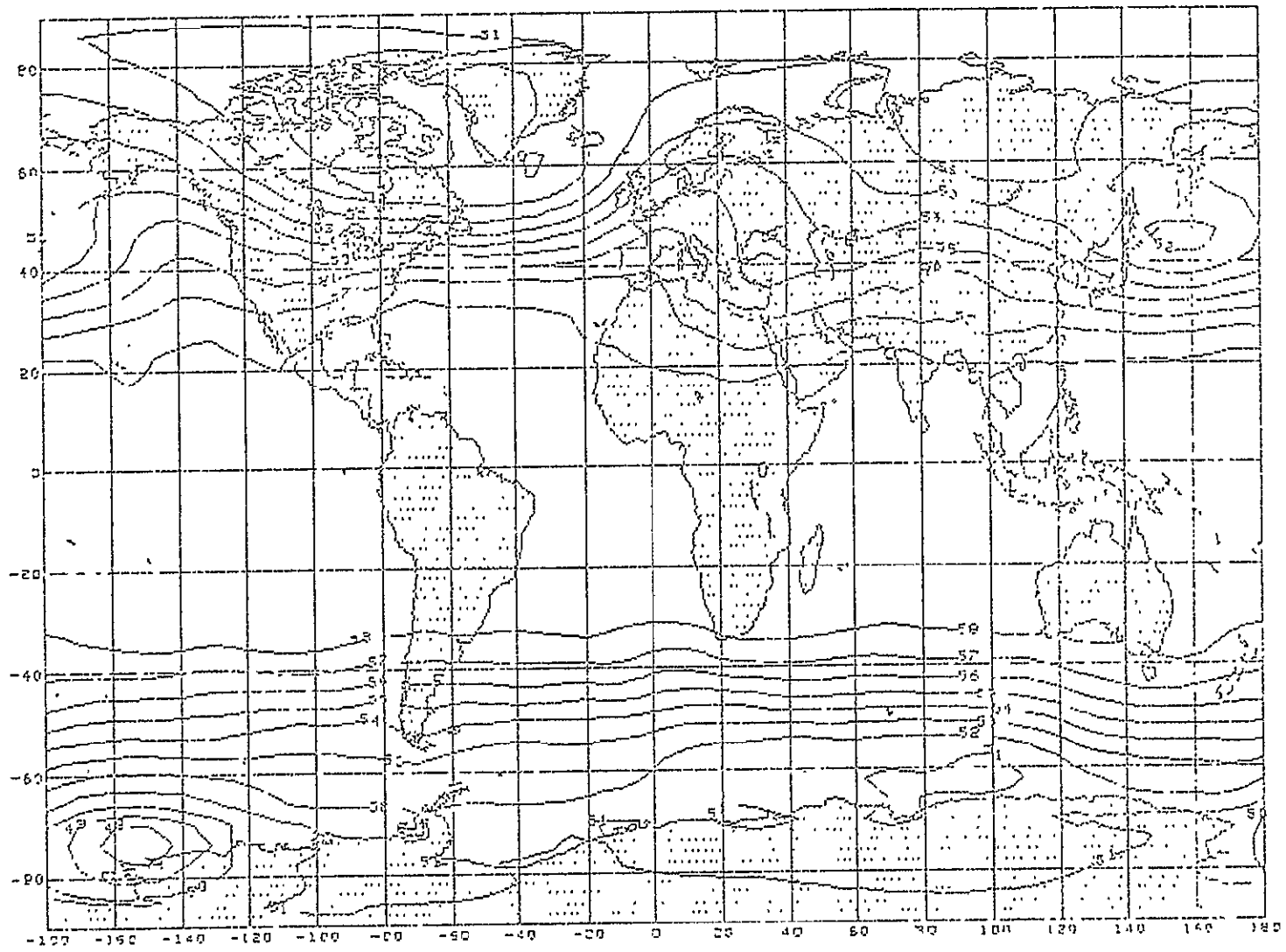

FIG. 16(0)

Table 7. (A) Root-mean-square (RMS) errors and (B) S1 skill scores of control (C) and anomaly (A) forecast mean sea-level pressure (mb) for January 1974. M and P denote climatology and persistence "forecasts", respectively. Minimum values are underlined.

A. RMS Error (mb)

Region	Forecast			
	C	A	M	P
Globe	<u>6.9</u>	<u>6.9</u>	7.6	9.2
Northern Hemisphere	<u>7.3</u>	7.4	9.2	11.7
Tropics	3.6	3.6	3.2	<u>1.9</u>
East Pacific-U.S.	<u>6.6</u>	<u>6.6</u>	9.3	12.4
North America	7.5	5.7	<u>5.5</u>	10.8
U.S.	5.5	4.6	<u>3.4</u>	9.5
Europe	8.3	<u>6.8</u>	15.5	10.1

B. S1 Score

	C	A	M	P
Globe	<u>69</u>	71	80	74
Northern Hemisphere	<u>67</u>	70	89	81
Tropics	<u>69</u>	70	80	60
North America	<u>89</u>	98	106	90
U.S.	<u>93</u>	99	101	97
Europe	70	<u>69</u>	110	95

Table 8. (A) Root-mean-square (RMS) errors and (B) S1 skill scores of control (C) and anomaly (A) forecast mean 500-mb geopotential height (m) for January 1974. M and P denote climatology and persistence "forecasts", respectively. Minimum values are underlined.

A. RMS Error (m)

Region	Forecast			
	C	A	M	P
Globe	<u>69</u>	74	88	93
Northern Hemisphere	<u>76</u>	83	108	116
Tropics	39	40	<u>25</u>	29
E. Pacific-U.S.	83	<u>81</u>	103	114
North America	90	85	<u>83</u>	151
U.S.	100	91	<u>80</u>	101
Europe	95	<u>92</u>	252	121

B. S1 Score

	C	A	M	P
Globe	<u>46</u>	49	55	58
Northern Hemisphere	<u>45</u>	49	60	64
Tropics	<u>65</u>	69	72	69
North America	<u>28</u>	35	43	57
U.S.	<u>23</u>	30	41	52
Europe	<u>57</u>	59	84	79

Table 9. Root-mean-square errors of control (C) and anomaly (A) forecast mean 850-mb temperature for January 1974. M and P denote climatology and persistence "forecasts", respectively. Minimum values are underlined.

Region	Forecast			
	C	A	M	P
Northern Hemisphere	<u>4.6</u>	4.7	5.1	4.7
E. Pacific-U.S.	5.6	5.1	<u>3.3</u>	6.3
U.S.	6.0	5.1	<u>4.0</u>	7.8

With regard to the impact of SST updating on rms error, Tables 7-9 are somewhat ambiguous. Over the large geographical regions (globe, tropical belt, and Northern Hemisphere) the C forecasts show no larger rms errors than the A forecasts in all three prediction variables, indicating no beneficial impact of the SST updating. However, over smaller regions ("United States", "North America", "Europe"), the rms errors are smaller for the A forecasts, suggesting some possible regional beneficial influence of SST updating. The S_1 scores, on the other hand, with only a minor exception (sea-level pressure over Europe) indicate that the C forecasts are superior to the A forecasts, and show no clearly beneficial effect of SST updating on the model predictions.

The one limited prediction experiment described above thus indicates that updating sea-surface temperatures did not result in any clear-cut improvement in forecast quality over a period of one month, either in the daily or monthly mean fields. Indeed, the impact of the SST anomalies on the prognoses was very slight. It must of course, be recognized that the SST anomalies in January 1974 were relatively modest in scale, magnitude, and persistence, and are not representative of the large, persistent, and broad-scale anomalies which are occasionally found over the oceans. However, in view of the inherent decay of predictability of atmospheric models, it is doubtful that a meaningful test of the impact of even very large SST anomalies, or of any other influence, can be carried out for a forecast period in excess of a few days until the predictive skill of the models is substantially increased. The difficulty in demonstrating statistical significance for the impact of SST anomalies against the background of meteorological "noise" with present-day general circulation models is well illustrated in the experiments of Chervin et al. (1976).

dicted map compared with the observed field, the amplitude of the predicted trough over the Black Sea region is too flat, and the closed circulation in the western Pacific is not predicted at all. On the other hand, the broad, flat, zonal current over the western hemisphere in January 1974, extending from the west coast of North America to the east coast of Europe, is simulated fairly well in the prognostic mean 500-mb map for 1974. The January 1975 500-mb forecast (Fig. 10) for the Northern Hemisphere is the most successful of the three in terms of both the error statistics in Table 4 and the synoptic mean maps. Phase agreement between the predicted and observed mean contours is good in middle latitudes, but less satisfactory in low and high latitudes. Major defects are found, however, north of Japan, where the trough amplitude is underpredicted, and east of Greenland, where the ridge amplitude is overpredicted.

In summary, the model generates a credible monthly mean prognostic map for the 500-mb level, and exhibits general predictive skill in excess of climatology and persistence, despite some obvious errors. At sea level the model is less successful, showing no general skill in forecasting the monthly mean sea-level pressure field, although it did succeed in reproducing the interannual changes in the depth of the mean January Icelandic low from 1973 to 1975.

4. SUMMARY AND CONCLUSIONS

The three January forecasts with the GISS model, using a fixed climatological SST field, have shown that, while the model is capable of simulating realistically the general structure and circulation of the mean troposphere, it fails to account satisfactorily for the observed interannual variations in either the monthly mean energetics or zonally-averaged circulation of the atmosphere. Thus, it must be concluded that the model is not yet capable of explaining the year-to-year fluctuations in the monthly mean state of the atmosphere on the basis of the initial conditions at the beginning of the month. Nor indeed has it been shown that the observed monthly mean state is in fact determined primarily by the initial conditions as defined by the large-scale analysis.

As a long-range forecasting system, the GISS model exhibits no general skill in predicting the monthly mean sea-level pressure field. However, the model did succeed in reproducing an observed interannual change in the depth of the mean January Icelandic low, which was weak in 1973 and 1975 and abnormally strong in 1974.

The model does appear to show consistent skill in forecasting the monthly mean 500-mb height field over the Northern Hemisphere. The three January monthly mean 500-mb forecasts are superior to climatology and persistence in terms of both rms errors and S1 skill scores, especially over North America, and the monthly mean prognostic maps compare favorably with the observed fields.

The use of daily updated sea-surface temperatures in the prediction for January 1974 produced no detectable beneficial effect on the forecasts, and, indeed, the total impact of observed versus climatological SST's on the evolution of the predicted large-scale atmospheric fields over a period of one month was very slight.

In the case of the sea-level pressure field, the decay of predictability of the model takes place so rapidly that, by the time the diabatic influence of the SST anomalies is felt by the atmosphere, all predictability has been lost, and no beneficial impact on monthly mean fields is demonstrable. At upper levels, specifically at 500-mb, where predictability decays less rapidly and the prognostic monthly mean fields appear to exhibit some skill over both climatology and perisitence, the physical impact of SST anomalies in the model is apparently so slight that again it is not possible to demonstrate any beneficial impact of the use of updated sea temperatures on the predicted monthly mean fields.

ACKNOWLEDGEMENTS

All the computations reported in this paper were carried out at and by the staff of the Goddard Institute for Space Studies. We wish to thank especially Robert Jastrow, director, Milton Halem, and William Quirk for providing space, facilities, and computing services at GISS for this study. Data were furnished by the National Meteorological Center and National Environmental Satellite Service of NOAA, and the U.S. Navy Fleet Numerical Weather Central. Gertrude Fisher drafted several of the figures. Joel Tenenbaum was especially helpful with regard to the energy computations, and William Quirk's guidance and advice on all phases of the data processing and computations was invaluable. Winthrop T. Johnson assisted in the final stages of the computations.

List of Figures

11. January 1974 sea-surface temperature (SST) anomaly (degrees C) based on satellite data provided by National Environmental Satellite Service (NESS), NOAA. (Anomaly is the observed deviation relative to the January mean SST field from Washington and Thiel, 1970.)

12. January 1974 sea-surface temperature (SST) anomaly (degrees C) in the Northern Hemisphere based on data provided by U.S. Navy Fleet Numerical Weather Central, Monterey, California.

13. January 1974 sea-surface temperature (SST) anomaly (degrees C) derived from merger of data in Figs. 11 and 12. (See text for details).

14. Growth of root-mean-square (rms) errors of predicted sea-level pressure (mb) over the Northern Hemisphere during first 3 weeks of January 1974. Dashed curve: C forecast. Solid curve: A forecast.

15. January 1974 mean sea-level pressure. Top (C): predicted with climatological SST's. Middle (A): predicted with daily updated SST's. Bottom (O): observed.

16. January 1974 mean 500-mb height. Top (C): predicted with climatological SST's. Middle (A): predicted with daily updated SST's. Bottom (O): observed.

References

Arakawa, A., A. Katayama, and Y. Mintz, 1969: Numerical simulation of the general circulation of the atmosphere. Proc. WMO/IUGG Symp. Numerical Weather Prediction, Tokyo, Japan Meteor. Agency, IV, 7, 8-12.

Arakawa, A., 1972: Design of the UCLA general circulation model. Tech. Report No. 7, Department of Meteorology, University of California, Los Angeles.

Baumhefner, D.P., 1970: Global real data forecasts with the NCAR two-layer general circulation model. Mo. Wea. Rev., 98, 92-99.

Bjerknes, J.A., 1966: A possible response of the atmospheric Hadley circulation to equatorial anomalies of ocean temperature. Tellus, 18, 820-829.

Chervin, R.M. and S.H. Schneider, 1975 (a): A study of the noise levels of climatological statistics generated by the NCAR GCM. (submitted to Journal of Atmospheric Sciences).

_____, 1975 (b): On determining the statistical significance of climate experiments with general circulation models. (submitted to Journal of Atmospheric Sciences).

Chervin, R.M., W.M. Washington, and S.H. Schneider, 1976: Testing the statistical significance of the response of the NCAR general circulation model to north Pacific Ocean surface temperature anomalies. (submitted to Journal of Atmospheric Sciences).

Crutcher, H.L. and J.M. Meserve, 1970: Selected Level Heights, Temperatures and Dew Points for the Northern Hemisphere. NAVAIR 50-1C-52. Naval Weather Service Command, Washington, D.C.

Druyan, L.M., 1974: Short range forecasts with the GISS model of the global atmosphere. Mo. Wea. Rev., 102, 269-279.

Druyan, L.M., R.C.J. Somerville, and W.J. Quirk, 1975: Extended-range forecasts with the GISS model of the global atmosphere. Mo. Wea. Rev., 103, 779-795.

Flattery, T.W., 1971: Spectral models for global analysis and forecasting. Proc. Sixth AWS Tech. Exch. Conf., U.S. Naval Academy, September 21-24, 1970. Air Weather Service Technical Report 242, pp. 42-54.

Halem, M. and G. Russel, 1974: A split-grid differencing scheme for the GISS model. Institute for Space Studies, Research Review, 1973, Part 2. Applications, pp. 194-200, Goddard Space Flight Center, NASA.

Leith, C.E., 1974: Theoretical skill of Monte Carlo forecasts. Mo. Wea. Rev., 102, 409-418.

Lorenz, E.N., 1973: On the existence of extended range predictability. J. Appl. Meteor., 12, 543-546.

Miyakoda, K., J. Smagorinsky, R.F. Strickler, and G.D. Hembree, 1969: Experimental extended predictions with a nine level hemispheric model. Mo. Wea. Rev., 97, 1-76.

Miyakoda, K., G.D. Hembree, R.F. Stickler, and I. Shulman, 1972: Cumulative results of extended forecast experiments. I. Model performance for winter cases. Mo. Wea. Rev., 100, 836-855.

Namias, J., 1953: Thirty-Day Forecasting: A review of a Ten-Year Experiment. Meteorological Monographs, Vol. 2, No. 6, American Meteorological Society, Boston, Mass. 83 pages.

_____, 1964: A 5-year experiment in the preparation of seasonal outlooks. Mo. Wea. Rev., 92, 449-464.

_____, 1971: The 1968-69 winter as an outgrowth of sea and air coupling during antecedent seasons. J. Phys. Ocean, 1, 65-81.

National Weather Service, 1974: A description of the Flattery global analysis method - No. 1. Technical Procedures Bulletin No. 105, January 10, 1974. National Weather Service, NOAA, Silver Springs, Md.

Oort, A.H. and E.R. Rasmusson, 1971: Atmospheric Circulation Statistics. NOAA Prof. Paper 5, Department of Commerce, Rockville, Md. 323 pages.

Oort, A.H. and J.P. Peixoto, 1974: The annual cycle of the energetics of the atmosphere on a planetary scale. J. Geophys. Res., 79, 2705-2719.

Peixoto, J.P. and A.H. Oort, 1974: The annual distribution of atmospheric energy on a planetary scale. J. Geophys. Res., 79, 2149-2159.

Posey, J.W. and P.F. Clapp, 1964: Global distribution of normal surface albedo. Geofisica Internacional, 4, 33-48.

Saur, J.F.T., 1963: A study of the quality of sea water temperatures reported in logs of ship's weather observations. J. Appl. Meteor., 2, 417-425.

Schutz, C. and W.L. Gates, 1972: Supplemental global climatic data. Report No. R-915/1-ARPA, 41 pages, RAND Corp., Santa Monica, Calif.

Shuman, F.G. and J.B. Hovermale, 1968: An operational six-layer primitive equation model. J. Appl. Meteor. 7, 525-547.

Smagorinsky, J., 1969: Problems and promises of deterministic extended range forecasting. Bull. Amer. Meteor. Soc., 50, 286-311.

Smith, W.L. D.T. Hilleary, J.C. Fischer, H.B. Howell and H.M. Woolf, 1974: Nimbus-5 ITPR experiment. Applied Optics, Vol. 13, 499-506.

Somerville, R.C.J., P.H. Stone, M. Halem, J.E. Hansen, J.S. Hogan, L.M. Druyan, G.Russell, A.A. Lacis, W.J. Quirk and J. Tenenbaum, 1974: The GISS model of the global atmosphere. J. Atmos. Sci., 31, 84-117.

Spar, J. and R. Atlas, 1975: Atmospheric response to variations in sea surface temperature. J. Appl. Meteor., 14, 1235-1245.

Stone, P.H., S. Chow, H.M. Helfand, W.J. Quirk and R.C.J. Somerville, 1975: Seasonal changes in the atmospheric heat balance simulated by the GISS general circulation model.

Tenenbaum, J., 1976: Spectral and spatial energetics of the GISS model atmosphere. Mo. Wea. Rev., 104, 15-30.